SCIENTIFIC VISUALIZATION OF N-DIMENSIONAL ATTAINABLE REGIONS

BY

THOMAS PETERKA
B.S., University of Illinois at Chicago, 1987

THESIS

Submitted as partial fulfillment of the requirements
for the degree of Master of Science in Computer Science
in the Graduate College of the
University of Illinois at Chicago, 2003

Chicago, Illinois

This thesis is dedicated to Melinda, Chris, and Amanda, whose unwavering support and encouragement helped make a distant dream become a reality.

ACKNOWLEDGEMENTS

I would like to thank the following people individually for their contributions to this work. Some are thesis committee members, others collaborators in one form or another. All were instrumental to the success of this thesis and I am deeply indebted to them.

- Andrew Johnson of the Electronic Visualization Laboratory (EVL), University of Illinois at Chicago (UIC) for helpful feedback and review of the thesis
- Jason Leigh, EVL, UIC for continued support and helpful input
- John Bell, lecturer, UIC. Dr. Bell tirelessly reviewed weekly progress, arranged collaborations, and was instrumental in the success of this work from start to finish. His enthusiasm, involvement, and high expectations helped this thesis become a truly meaningful endeavor.
- Peter Nelson, CS department head, UIC, for ongoing overseeing of the work
- Tumisang Seodigeng, researcher, Center of Process and Material Synthesis, School of Process and Materials Engineering, University of Witwatersrand, Johannesburg, South Africa. Mr. Seodigeng was most helpful with the second sample problem, and was our collaborator in the field doing actual AR research. I am thankful not only for his data set, but for the invaluable feedback as well.
- David Glasser, and Brendon Hausberger of the University of Witwatersrand, Johannesburg, South Africa also for their collaboration on the second sample problem.
- Ken Clarkson, researcher, Bell Labs, Murray Hill, New Jersey. Mr. Clarkson generously provided an open-source application for computing convex hulls in general numbers of dimensions. His code was very reliable, and it played a valuable role in the visualization of the second sample problem.

TP

TABLE OF CONTENTS

TABLE OF CONTENTS (continued)

LIST OF TABLES

LIST OF FIGURES

FIGURE PAGE

LIST OF ABBREVIATIONS

2-d, 3-d, 4-d, n-d	2-dimensional, 3-dimensional, 4-dimensional, n-dimensional
AR	attainable region
CAVE	CAVE Automatic Virtual Environment
CG	computer graphics
CRT	cathode ray tube
CSTR	continuous stirred tank reactor
DSR	differential side stream reactor
EVL	Electronic Visualization Laboratory
GUI	graphical user interface
LCD	liquid crystal display
MFC	Microsoft Foundation Classes
MVC	model view controller
PC	personal computer
PFR	plug flow reactor
RAM	random access memory
UIC	University of Illinois at Chicago
VR	virtual reality

SUMMARY

The attainable region (AR) is a graphical method for solving chemical reactor synthesis problems. Geometrically, it is a closed convex solid in n-dimensional space and it represents the solution space of all possible combinations of concentrations that can be produced by a given chemical system, starting with a given feed stock. Even though a set of unit operations can be combined in an infinite number of ways through series, parallel, bypass and looping, all possible resulting concentrations are contained in the AR. The number of dimensions of the space, n, is the same as the number of components in the chemical system.

AR is a field currently being studied by several teams of researchers in selected institutions worldwide. A survey of their literature together with collaboration with one group from the University of Witwatersrand in South Africa reveals that scientific visualization of AR results becomes increasingly difficult as ARs reach higher dimensions. Generic visualization tools with limited dimensional capability have proved inadequate. A scientific visualization tool specifically designed for AR data with the capability to dynamically select subsets of dimensions as well as the ability to view all n dimensions simultaneously is needed.

In this thesis, thorough background research in AR is performed, the current state of AR visualization is assessed, and then an application is developed for scientific visualization of n-dimensional (n-d) AR data. Principles of interactive computer graphics, virtual reality, user interface design, and multivariate scientific visualization are employed in a real-time viewer capable of reading n-d AR input data and selectively producing various views via dimension reduction, tetrahedral coordinates, convex hull generation, and a standard input file format.

Other program features include interactive data probing, coordinate system controls, real-time viewing transformations, and a functional user interface. The application is a freely available open-

source program that runs on most personal computers (PCs) under most versions of the Windows operating systems. Virtual reality devices such as the CAVE, tiled display, and auto-stereoscopic display have been examined as part of the background study, and feasibility for future migration of the application to these devices is assessed.

Two sample problems are documented, the first theoretical and the second an actual data set from current AR research. Collaboration with researchers has helped the application to evolve, and the program and results have been shared to help guide researchers in further studies. Preliminary feedback from collaborators has been positive. The overall contribution of this thesis is to provide an interactive visualization tool for n-d ARs, which is needed to help AR research move to higher dimensions.

1. INTRODUCTION

Chemical engineering, like other engineering disciplines, often relies on graphical methods for solving complex problems. This works well for “textbook” problems, but unfortunately graphical methods are difficult to apply to many "real" problems because they are often much more complex. The increased complexity is due to increased number of variables, ie. larger dimensional space. For example, sample graphical problems are usually two-dimensional, while real problems may contain 5 or 10 variables. However, graphical solutions offer advantages over other numerical methods because of the visual perception of the human mind, so graphical solutions for multivariate problems are desirable. While it is difficult to visualize high dimensional data, a good visualization will reward the engineer with extremely comprehensible results.

One such graphical method in chemical engineering is called "attainable regions", or AR. This is a geometric representation of the solution space of all possible combinations of selected unit operations for a system of chemical reactions, starting from a given feed point. The chemical engineer desires to find an optimal flowchart combination of reactors and mixers to optimize some objective function, such as production of a desired component, and the first step in this optimization process is to determine what compositions are feasible, or attainable. The attainable region is a convex closed solid in n-dimensional space, where n is the number of components in the chemical system.

The following example will serve to introduce ARs, especially to those readers with backgrounds other than in the field of chemical engineering. Suppose that an engineer is charged with the task of designing a new chemical plant consisting of a set of chemical reactors and mixers to operate on some given chemical system such as below. (van de Vusse, 1964)

$$A_1 \rightarrow A_2$$

$$A_2 \rightarrow A_4$$

$$2A_1 \rightarrow A_3$$

Usually the goal is to maximize some objective function, for example maximizing production of A_4 while minimizing the number of reactors used. The engineer also has a set of fundamental operations to choose from. In this thesis, 4 ideal operations are considered: 3 types of reactors and bulk mixing. Each of these can be described by an ideal model governed by a differential or algebraic equation. The difficulty lies in the fact that the unit operations can be combined in an infinite number of ways using series, parallel, bypass, looping, etc. For example, Figure 1 below shows a small flowchart of several reactors connected together.

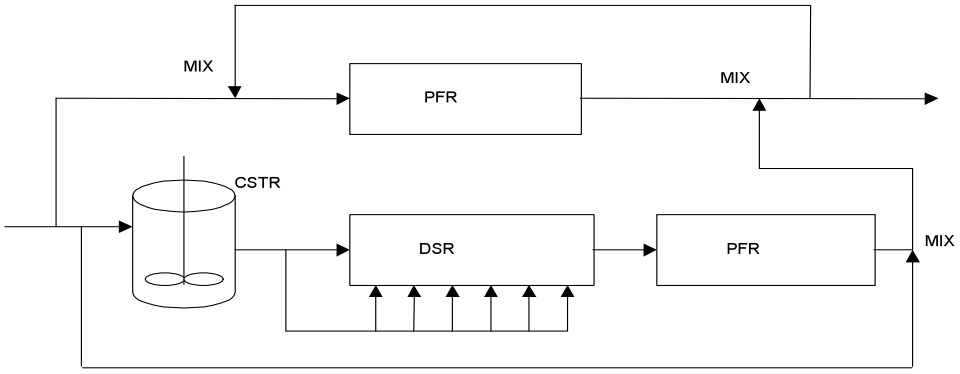

Figure 1. Sample process flowchart

Since the number of combinations of processes is infinite, the engineer has two choices. Either he may reduce the number of possibilities by applying heuristics, rules of thumb, or historical experience, or apply a more systematic scientific method. Obviously the latter is preferred, and ARs provide this method. The AR is easy to visualize when the number of dimensions is small, say two or three, but difficult to visualize when higher dimensions are used. Not surprisingly, it is just these high-dimensional (high-d) ARs that occur in real-life chemical engineering situations, as opposed to low-d "textbook" examples.

A survey of AR literature reveals that the current state of AR visualization follows two patterns. Either the number of variables visualized is reduced (for example from 5 down to 2 or 3), or high-d results produced by numerical methods may not be visualized at all. (See Section 2.4.6 for more details.) The whole basis for the AR method first invented by Horn (Horn, 1964) is to see the space of *all possibilities*, which then can lead to rational optimization paths. A useful n-d visualization tool specifically designed for AR data can eliminate the necessity to discard variables, and provide a visualization of data where there was none before.

A collaboration was formed with a key research group currently pursuing the study of high-d ARs. A working partnership with the University of Witwatersrand, in Johannesburg, South Africa was begun and a need was discovered for high-d visualization of AR results. A scientific visualization program was developed as part of this thesis work which can interactively produce views based on dimension reduction, tetrahedral coordinates, and convex hull generation. Other features include data probing, real-time viewing transformations, and a functional user interface including online help. Through the use of a standard file format (also developed as part of this thesis), researchers are able to focus on what they do best, simulating and producing data sets, freeing them from developing visualization methods.

Two sample problems were tested, 4-dimensional and 5-dimensional, and the application is designed to accept even larger problem spaces. Concepts from several different disciplines are employed, from chemical engineering, scientific visualization, and computer science. Chemical engineering provides the basis for the AR method of modeling reactor synthesis, while concepts from the study of scientific visualization to graphically represent high-d data are utilized to maximize comprehension. Finally, several topics in computer science are explored to develop the computer application that serves as the visualization tool, such as 3-d computer graphics, virtual reality, and user interface design.

The following is a list of specific enhancements or additions that this thesis contributes to the current state of AR visualization. The following chapters provide background and detail as to how this was accomplished.

- Providing an interactive AR-specific visualization tool capable of maintaining all dimensions of a problem space and selectively displaying a subset of dimensions under various settings as well as displaying all dimensions simultaneously if desired
- Applying the tetrahedral coordinate system to AR visualization, which does not appear in any AR literature as yet but is a useful display paradigm for chemical engineers and researchers
- Using n-d and 3-d convex hulls to view disorganized data sets and to filter extraneous data from large data sets prior to viewing, allowing these data to be viewed as well
- Developing a standard file format for the transmission of data sets between simulation programs and the visualization, enhancing communication of results between research organizations

2. BACKGROUND

A synthesis of concepts from the studies of AR, scientific visualization, and computer science form the background material for the thesis. Computer science topics include a discussion of computer graphics, virtual reality, and user interface design. Scientific visualization, specifically multivariate visualization is explored in order to display higher numbers of dimensions within a limited dimensional space. ARs are researched in order to understand AR theory, properties and features of the AR, and the current state of visualization in this domain.

2.1 Computer Graphics and Virtual Reality

3d computer graphics (CG) is the rendering of objects in three-dimensional world-space onto a two-dimensional computer display device; typical applications are computer aided design, user interfaces, games, and artistic expression. Virtual reality (VR) is an extension of 3d computer graphics through specialized software and hardware for the purpose of creating a sense of immersion in the computer application. The list of applications suitable for VR is similar those for CG. Sherman and Craig define VR as: “a medium composed of interactive computer simulations that sense the participant’s position and actions or augment the feedback to one or more senses, giving the feeling of being mentally immersed or present in the simulation (a virtual world).” (Sherman and Craig, 2003)

This is a specific textbook definition that also enumerates some key ingredients of VR, namely position tracking, sensory feedback, and immersion. CG and VR are considered together in this thesis as they relate to scientific visualization with the aim of maximizing data comprehension. What follows is a very brief introduction to some common CG/VR display devices and systems as they relate to the AR visualization. Some devices such as the CAVE are where the work began, others such as laptops and PCs are the current platform, and still others such as tiled displays and auto-stereo displays are the future intended targets for the AR work.

2.1.1 **CAVE**

The CAVE, or CAVE Automatic Virtual Environment, was invented at the Electronic Visualization Laboratory (EVL) at the University of Illinois at Chicago (UIC) in 1992. (Cruz-Neira et al., 1992) It is a 10-foot x 10-foot x 10-foot cube in which several participants can stand simultaneously. Viewers are surrounded by three walls of rear-projection screens, and together with the floor, this constitutes four surfaces onto which images are seamlessly projected through the use of high quality projectors and mirrors. Images are projected in field-sequential stereo, meaning that images alternate between left and right eyes through the use of synchronized LCD shutter glasses to create a stunning 3d effect. One viewer's position is tracked through an ultrasonic tracking system, and the viewpoint is updated in real-time to maintain first-person perspective. Finally, a high quality sound system is included.

For over ten years, the CAVE has represented the state-of-the-art in high-end VR technology. The CAVE was the first choice for the AR visualization because of the 3d stereoscopic immersive experience it provides. It was thought that such high-end VR equipment would enhance the viewing of high-d data. In Section 3.2, it will be shown that this assumption was not necessarily true, and actually the CAVE had some drawbacks that ultimately resulting in the use of other devices. Figure 2 below appears on the EVL web site (EVL, 2003) and diagrams the CAVE architecture of screens, mirrors, and projectors.

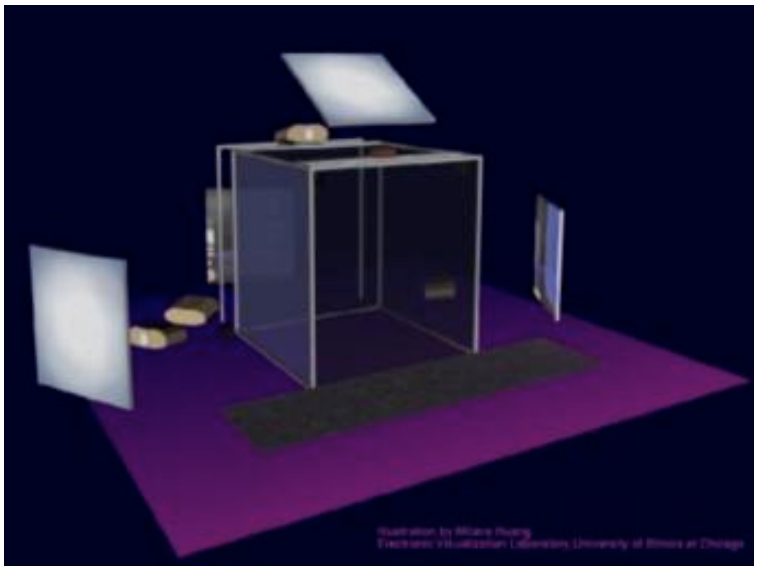

Figure 2. CAVE architecture (image courtesy of EVL)

2.1.2 **Tiled Displays**

For years, VR technology was primarily either projection-based or head-based. Only recently has a third display option emerged: tiled. A tiled display is a matrix of smaller individual displays, driven by a cluster of PCs, and assembled to make a large-size, high resolution, high brightness, wide field of view display. The individual components can be either liquid-crystal display panels (LCDs) or projectors. EVL at UIC has been one of the innovators of the LCD tiled display, with their “Perspectile” model. (JuxtaView, 2002). Shown below, the system displays a total resolution of approximately 6000x3000 pixels and enables researchers to quickly pan and zoom through very large data sets, often terabytes in size. Also, not all of the tiles need to show parts of the same image, so that several applications or several views of a data set can be viewed simultaneously. All of the above features make tiled displays a likely future candidate for scientific visualization such as the AR work.

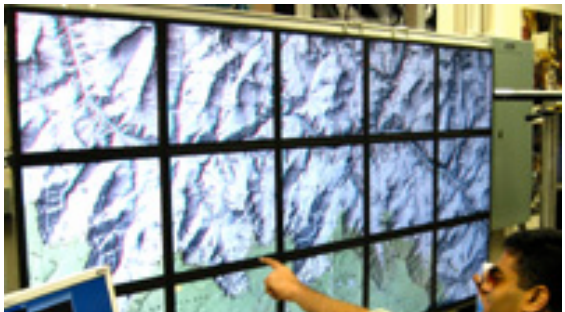

Figure 3. Tiled LCD display (image courtesy of EVL)

Another variety of tiled display uses a collection of projectors to form an even larger viewing space for research, presentation, or educational purposes. This is the approach taken at Vrije Universteit in the "ICWall" tiled display, composed of eight projectors. (Renambot and van der Schaaf, 2003) Each tiled method has its pros and cons. The LCD display is relatively portable and economical, but suffers from the borders that surround each tile, or mullions. The projector display is large and relatively seamless, but requires a dedicated space and permanent installation. Figure 4 below is used with permission from Luc Renambot. (Renambot and van der Schaaf, 2003)

Figure 4. Tiled projector display (image courtesy of Luc Renambot)

2.1.3 **Auto-Stereoscopic Displays**

One of the drawbacks of current VR technology is the need for various encumbrances that the user must wear in order to achieve effects such as tracking and stereo vision. Head mounted displays, tethered tracking devices, LCD shutter glasses, even passive stereo red-blue filter glasses are all examples of such paraphernalia that are still required today to create a feeling of immersion and a sense of presence in virtual worlds. Unfortunately, these items can be uncomfortable, restrictive, and detracting from the experience, especially after long periods of use. VR researchers have long been dreaming of a system where a user simply walks up to a display and is presented with stereo sights and sounds, totally unencumbered by additional devices.

In recent years, one of the research projects at EVL has been the development of the "Varrier" display, an auto-stereo display based on physical and virtual barrier strip technology. (Sandin et al., 2001) Present development is underway for a 4-panel system, although future plans are to incorporate the Varrier technology on a larger tiled display such as the Perspectile 15-panel system mentioned earlier. Concurrently, EVL is also conducting research in camera-based head tracking, so that the system can know the user's position at all times without having to wear a tracking device. In the photograph below, the researcher is still are wearing a head-tracker mounted on a headband, but the overall goal is the permanent elimination of all such impediments. Varrier is also a likely candidate for future AR visualization, because of the active stereo feature and the multi-panel capability of displaying several views simultaneously. While it offers wide field of view, the system suffers from lower resolution and brightness due to the physical linescreens covering the panels. Artifacts such as ghosting also are still a problem, but are being reduced through ongoing development.

Figure 5. Auto-stereo 4-panel display

2.1.4 **Desktop Displays**

Finally, one should not overlook the most ubiquitous graphics display, the common everyday PC desktop or laptop CRT or LCD display. Sometimes called “fishtank” VR, it is possible to produce a tracked, stereo VR experience on an ordinary desktop computer monitor, although it is uncommon to expend the additional effort for such a small display. What is common however, is simply displaying 3d computer graphics applications driven by commodity PC graphics cards on an ordinary monitor, without any extra effort. Most computer users do this everyday without giving it a second thought when using graphical user interfaces or running computer games. One can hardly call this VR, but considering the relative numbers and costs of PCs compared to CAVEs or other dedicated equipment, the obvious conclusion cannot be ignored. The PC monitor is *the* predominant computer graphics display media, especially since it can easily be coupled with a projector for wall-sized displays and presentations. This became one of the major factors in the choice of current application platforms for this work.

2.2 User Interface Design

User interface design is the study of developing applications to be usable by other people than just the author of the program. As Andrew Johnson writes, “Making a program work for you is pretty easy. Making it work for another user is much harder.” (Johnson, 2002) User interfaces are not limited only to computer applications either; they are all around us in everyday life as well, (Norman, 1988) but this discussion will be limited to a brief summary of “user centered design” as it pertains to this visualization. It is interesting to note that some of the goals of interface design are similar to those of scientific visualization. In a broad sense, the visualization is an *interface* to the underlying data, much the same way as widgets and controls are an interface to a computer application.

The following is a brief outline of some of the guiding principles of user centered interface design, especially as they pertain to the application in question. This section is condensed from an entire semester-long course, and the interested reader is encouraged to consult any number of user interface texts, such as Schneiderman. (Schneiderman, 1998)

2.2.1 Transparency

The first and probably most important characteristic of a good user interface is transparency. In other words, the best interfaces are the ones the user never sees. In a perfect world, the user concentrates only on the task at hand, in this case the attainable region, and never thinks about which menu item or dialog box is needed or where that option is documented in the online help. Such a perfect application has yet to be developed, but every now and then some individual feature is implemented well, and its use becomes transparent.

2.2.2 **Direct Manipulation**

A closely related concept is direct manipulation. The more directly an action can be done, the more transparent it will become. In this context, the word “direct” means simple, concise, or most closely affording the intended result. This is what makes the “drag-and-drop” metaphor so attractive in windows desktop systems, for example dragging a file icon to the trash icon in order to delete it. A distinguishing feature of direct manipulation is direct feedback, much like the way a car is driven. One does not think, “I will now turn the steering wheel 35 degrees to the right.” Rather, the driver turns the wheel slightly and the result is immediately sensed. Then the driver turns more, etc., performing a rapid series of incremental motions and adjustments while the task is smoothly executed. When direct manipulation occurs so easily that it requires little or no conscious thought, it again becomes transparent.

Navigation within the AR visualization is designed with this in mind. Real-time panning, zooming, and rotating are accomplished using the wand in the CAVE version and the mouse in the PC version. In the CAVE, the user points the wand in the desired direction of travel and manipulates the joystick or trackball to control the speed of the motion. In the PC version, dragging the mouse with the right mouse button depressed along with shift and control keys accomplishes the same result. Both methods are easy to learn, and become transparent quickly. Both offer direct manipulation and feedback, with sensitive speed control.

2.2.3 **Building Tools**

Microsoft foundation classes (MFC) within the Visual C++ environment provide tools for constructing standard window controls such as menus, dialog boxes, toolbar buttons, and icons in an application. There are other similar tools and libraries such as Borland C++ Builder, FLTK for Linux, but the choice of particular tool is not the point. The idea is that the use of building tools is necessary

in modern user interface development. It affords rapid prototyping and the resulting interface is uniform across the application and similar to other applications the user is already accustomed to. What follows are a few examples of how a building tool such as MFC helped standardize the AR visualization.

Window controls, menus, toolbar, icons

Included are standard drag-able title bar, minimize, maximize, close buttons, and re-sizable borders. A status bar appears at the bottom with several panes to display file name and useful messages. The main menu is straightforward with only two levels of depth, and a toolbar appears below the menu with several icons for the common menu operations. See Figure 6 below.

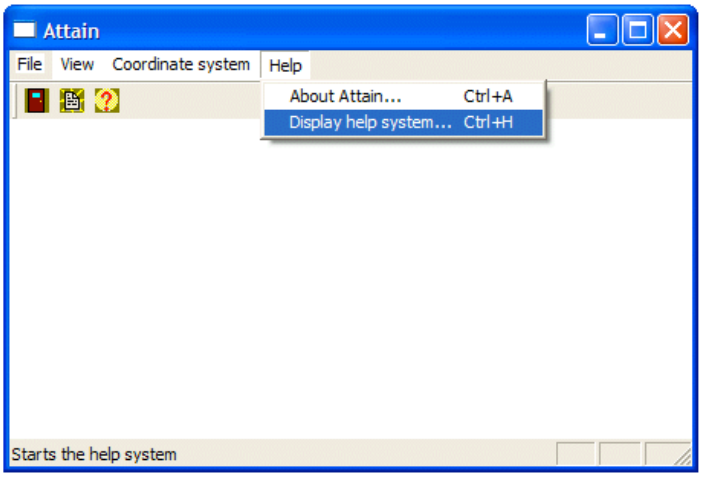

Figure 6. Basic window elements

Dialog boxes

Dialog boxes are used to display information and to receive user input, as in the setting of various options. The dialog shown below at left is the opening “splash” screen when the application starts up, and is also used as the “help | about” screen. On the right is the scale values dialog box, an example of a dialog used to set user options.

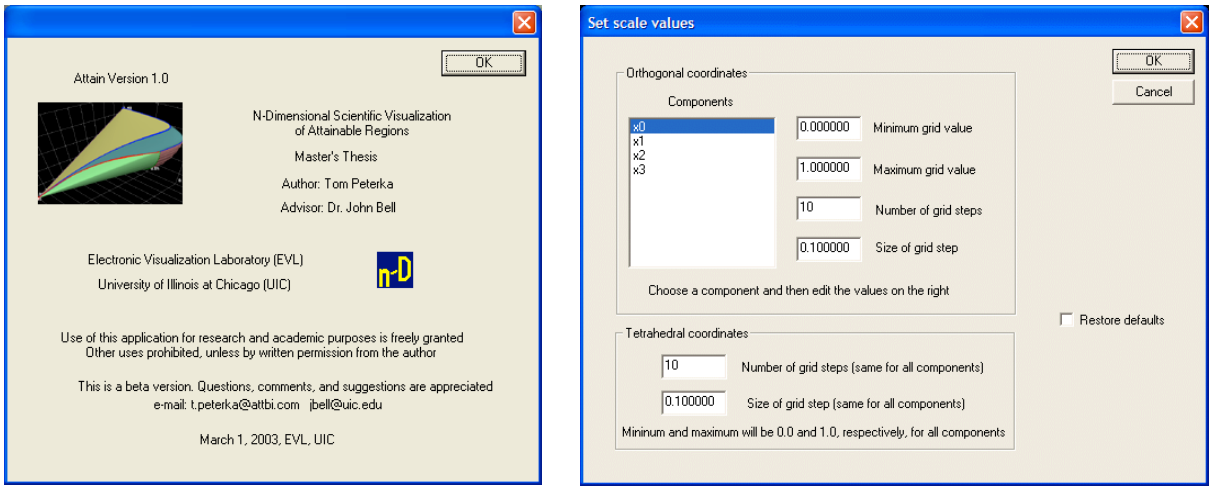

Figure 7. Examples of dialog boxes

Help

A help system is included with documentation on all menu items and dialog box controls. It also is standardized to look and function like the help systems from other Windows applications with which the user may already be familiar. It includes contents, an index, and a search command.

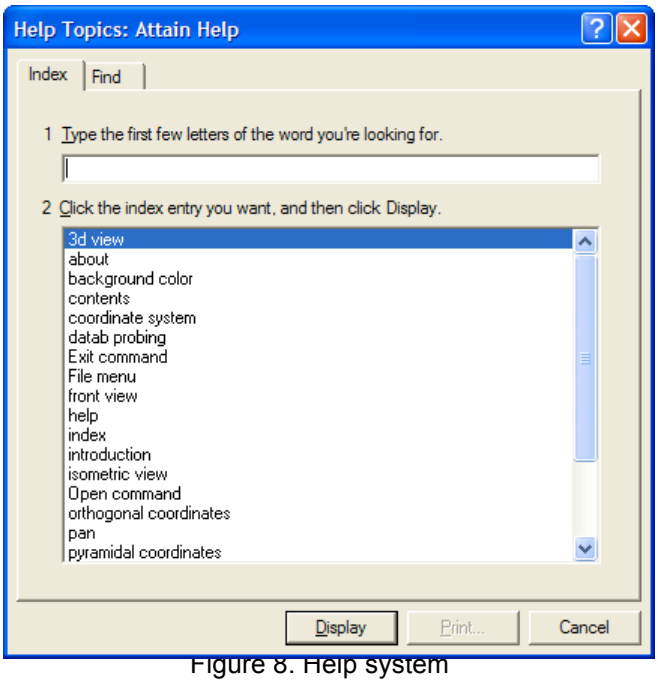

Figure 8. Help system

2.2.4 **Color**

The effective use of color can be a tricky business. In a word processor or spreadsheet, color is often used only as a highlighting mechanism, so it is easy to be conservative and use only 2 or 3 colors total. Other applications, especially scientific visualization, require a broad color spectrum because color often conveys additional information such as an extra variable. (Nielson et al., 1997) Unfortunately, color is also easy to misuse, resulting in color combinations that are difficult to see (eg. red next to blue), unwanted meanings, or just plain unsightly displays. The opposite extreme is equally bad: the over-use of color in order to produce an aesthetic display can mask the data's true meaning, the "pretty picture syndrome". Finally, approximately 8 percent of men and .5 percent of women are color-blind to some degree, making color even more difficult to use well.

In the AR visualization, color is used for background, text, gridlines, points, curves, and surfaces. Rather than being used as a variable such as temperature, surface color is used as an identification attribute to distinguish various parts of the AR that are produced by different chemical reactors and mixers. Figure 9 below is an example of three different surfaces, corresponding to distinct processes.

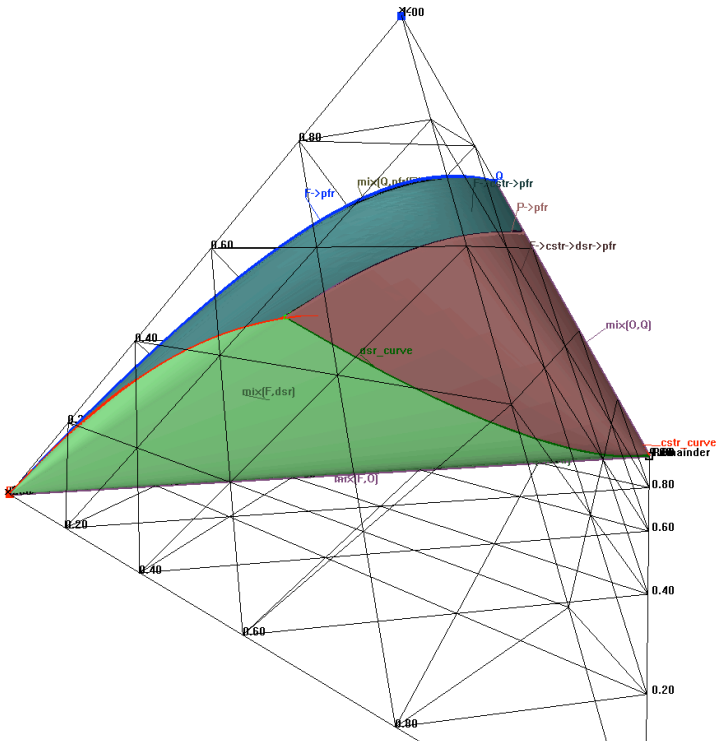

Given the aforementioned difficulties in color selection, it becomes impossible to find color combinations to satisfy everyone. So, the best policy is to let the user decide. Background and text default to black and white respectively, but are selectable through color selection dialog boxes. Other colors of geometric data objects are set through the input data file, documented in Appendix A. This strategy is the best compromise to the color problem.

2.2.5 **Testing and Evaluation**

Testing and evaluation are major factors in user interface design, and the key is to test early and often, rather than as an afterthought when the application is complete. The current state of the work was reviewed on a weekly basis, so there were many opportunities to experiment and refine. Also, our colleague, Tumi Seodigeng from the University of the Witwatersrand in Johannesbug, South Africa, was supplied with several beta versions of the program, and provided input via e-mail. Evaluation was largely informal, with comments and suggestions being implemented along the way. Unfortunately, time did not allow for more formal techniques to be used on larger test groups of users.

However, a survey form to be used in the future as an evaluation instrument is included in Appendix C.

2.3 Scientific Visualization

2.3.1 General Principles

Scientific visualization has its roots in the latter part of the eighteenth century with the graphs of William Playfair, first published in 1786. (Tufte, 1983) It is not a new study, and goes by several names including data visualization and data graphics. The goal of good visualization is to depict data visually, graphically, or pictorially as opposed to only listing tables of numbers, in order to maximize data comprehension. The old maxim, “A picture is worth a thousand words” applies here, as most people recognize patterns and relationships graphically easier than numerically. Over the course of 200 years or so, the discipline matured, and it became clear what comprises good quality, high-content data graphics, at least in two dimensions on ink and paper.

Then, like so many areas, the field of scientific visualization was turned upside-down with the advent of computer graphics, moreover with the availability of fast, cheap computer graphics hardware. Computer-generated graphics began to be churned out at an amazing pace and with incredible ease. Today, anyone who can enter numbers into a spreadsheet can produce printer tray-fulls of charts and graphs in a matter of minutes. Of course, it is just as easy to produce bad, useless, data-thin, and even nonsensical graphs at the same incredible pace. One does not have to look far to find them either, usually a quick glance at any mass-produced news media will do.

Edward Tufte has written three excellent volumes on the study of data visualization, and he devotes considerable effort characterizing the differences between good and bad graphics. (Tufte, 1983; Tufte, 1990; Tufte, 1997) What follows is only a brief list of some of his salient points.

According to Tufte, excellent graphics should:

1) show the data

2) encourage the viewer to focus on substance rather than design (transparency)

3) not distort the data (truthfulness)

4) present much information in a small space (high data density)

5) make large data sets coherent

6) encourage the drawing of comparisons and conclusions about the data

7) reveal several levels of detail, from broad to fine

8) display complex ideas with clarity, precision, and efficiency

9) display large numbers of variables (multivariate)

Tufte does a superb job elaborating on all of the above points and many others in his works and the reader is encouraged to explore his volumes. The effort will be rewarded with a comprehensive and interesting study of the history and theory of data visualization.

To repeat a previous concept, it is interesting to compare good interface design and good visualization. Some points are identical: transparency, levels of detail, simple presentation of complex ideas. Other aspects are specific to one topic of the other. Finally, in computer graphics scientific visualizations, a widget or control or graphical element (eg. a button or dialog box) belongs both to the user interface and to the visualization, so the topics become even more inter-twined. In this sense, visualization is a broader concept than just the end-result graphic produced by the program. Rather, visualization is the *process* of interacting with the data to producing desired and meaningful views of the data, resulting ultimately in comprehension of the data.

2.3.2 **Multivariate Visualization**

The goal of this visualization research is to effectively display multivariate data (n-d) on a 2-d device such as a computer screen, projection panel, or other VR or CG display medium. Keep in mind that even 3-d computer graphics are still ultimately shown in 2-d, it is only our minds that are "fooled" into thinking that we are seeing 3-d, since computer monitors and VR projection hardware still consist of flat 2-d devices. So how do we "escape flatland", as Edwin Abbot wrote over 100 years ago? (Abbott, 1952; first published in 1884)

2.3.3 **Dimensional Attributes**

The first method to "squeeze" extra variables into a limited variable-space is to use other attributes besides position to code additional data (Nielson et al., 1997). Probably the best-known example is the familiar weather map seen daily in the newspaper or on the evening news.

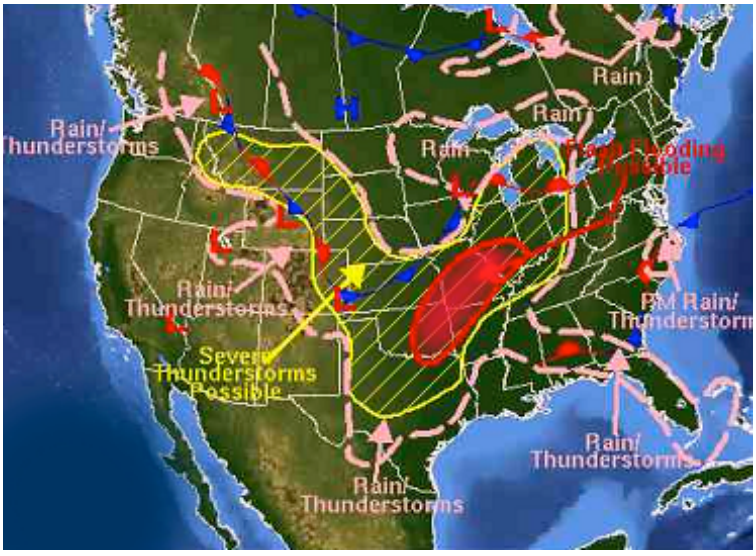

Figure 10. Daily weather map

In Figure 10, 2-dimensional position is given by the (x,y) location of a point on the map. Since this is a 2-d graphic, no further positional variables can be displayed. So other attributes such as color, shading, texture, annotations, etc. are used to extend the dimensional space beyond two dimensions. Below is a slightly more complex example of the same idea.

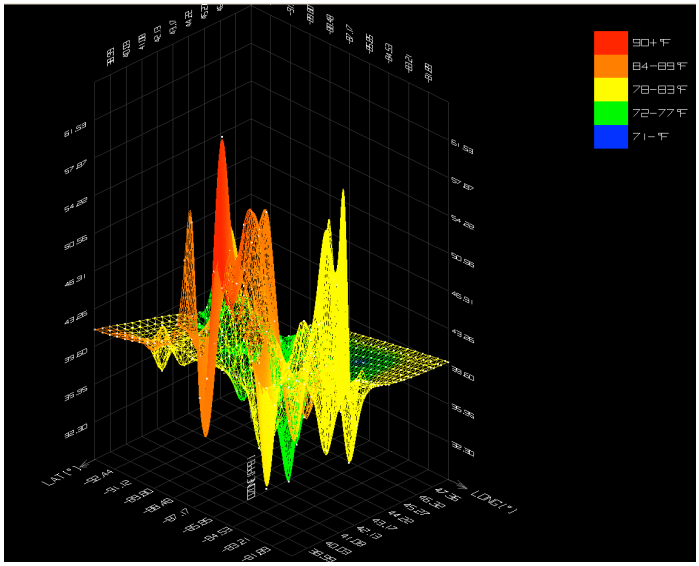

Figure 11. Air quality visualization (courtesy Mike Rizzo and Tom Peterka)

Figure 11 is from an earlier project by the author and a partner from the U.S. Environmental Protection Agency. The goal of the visualization was to search for a relationship between air temperature and air quality, specifically ozone levels. This view compresses four dimensions onto a 2-d computer screen. Three spatial dimensions are projected onto the 2-d display, and color is coded for the fourth dimension. Specifically, (x,y) indicates the position along the earth in longitude and latitude, z indicates ozone level, and color indicates temperature.

2.3.4 **Animation**

What Tufte calls “narratives of space and time,” (Tufte, 1990) is often called animation. When time is one the variables, real-time computer graphics provides a direct and natural way to display it: to

show a “movie.” This is especially effective when the scene complexity and graphics hardware is such that an acceptable frame rate (20-30 minimum frames per second) can be maintained so that smooth motion results. To continue with the previous example, if ozone and temperature were displayed across space and time (several hours, days, months, etc.), the display could be animated by producing a time-series of individual snapshots as shown above, and played back along with a clock display or time counter. The result would be compressing 5 dimensions down to 2.

2.3.5 **Dimension Reduction**

Multivariate display options are limited when there are multiple dimensions that cannot be codified intuitively using animation, color, texture, or other display attributes. This is the nature of the problem in the AR work. All dimensions in the problem space are spatial, and moreover the user will be evaluating the AR based on geometric characteristics. Of particular importance is that an AR must be convex, and the user will be looking for convexity in any of the produced views. Therefore, coding spatial dimensions with color or other attributes is not useful. This leaves only one option: to view a subset of dimensions at a time. Tufte calls this strategy “multiples”; (Tufte, 1997) the term used here is dimension reduction, whereby the number of dimensions is reduced to three or four at any one time.

In dimension reduction, two strategies can reduce the dimensions of a space. One may either project the data to the lower dimensional system, or create a cross-section through the data. A simple example reducing three dimensions down to two will make this clear. Suppose a sphere in 3d is to be projected to 2d. The result is essentially a top-down view of the sphere, a circle whose diameter is the same as the diameter of the sphere. On the other hand, in a cross-section, a sectioning plane is specified and the resulting view will be the intersection of the original model with the section plane. Continuing with the sphere example, the result will be a circle again, but probably a smaller diameter than the sphere depending on the position and orientation of the section plane. In the general n-d case, the original model is n-dimensional and a subset of dimensions is viewed via projection or

section. The section plane becomes a hyper-plane, or a higher dimensional plane formed by fixing various coordinates at specific values. Higher dimensional entities are discussed in more detail in Section 2.3.7.

2.3.6 **Coordinates and Coordinate Systems**

Without coordinates, a visualization is nothing but a pretty picture. It is the assigning of coordinate values that quantifies a data set and permits its visualization. There are many types of coordinate systems, not just the familiar Cartesian. For example, logarithmic, polar, spherical, parabolic, etc. are all possibilities. The choice of a coordinate system is not arbitrary; there are two reasons for choosing one over another for a given application. First, a system may naturally lend itself to the data and simplify the problem. For example, certain problems are much easier to solve in polar or spherical coordinates because the equations are simpler and the number of coordinates fewer.

The other factor is comprehension. The real goal of scientific visualization is to tell a story about the data (Tufte, 97). Data for its own sake is worthless; the value is in conclusions that are drawn, inferences made, comparisons generated. The choice of coordinate system is critical because patterns can become clear in one system that were obscured in another, just as a constant growth rate pattern may not be obvious on a linear scale but takes the familiar straight-line form on a logarithmic scale.

Besides the type of coordinate system, scale ranges and resolutions are also critical. If the goal is to tell a story about the data, the interesting parts may be missed by looking in the wrong places, not looking closely enough, or looking too closely and “missing the forest for the trees”. This is all a matter of setting appropriate scale ranges and scale steps.

In the AR application, two types of coordinate systems are utilized to plot chemical concentrations and mole fractions. Cartesian coordinates are used in 3-d concentration space, where concentration is measured in amount per unit volume, such as moles per liter. The second coordinate system is called “tetrahedral coordinates”. Here the plotted values are mole fraction rather than concentration, and there are no units because the measurement is a fraction of the desired concentration to the whole. The tetrahedral system is an extension of the ternary diagram, a familiar paradigm for chemical engineers where each of 3 components is plotted at the vertices of an equilateral triangle. All coordinates of a given point must add to 1.0, and since the dimensions are not independent, one extra coordinate may be “squeezed” into the view, resulting in 3 items on a 2-d graph as shown below.

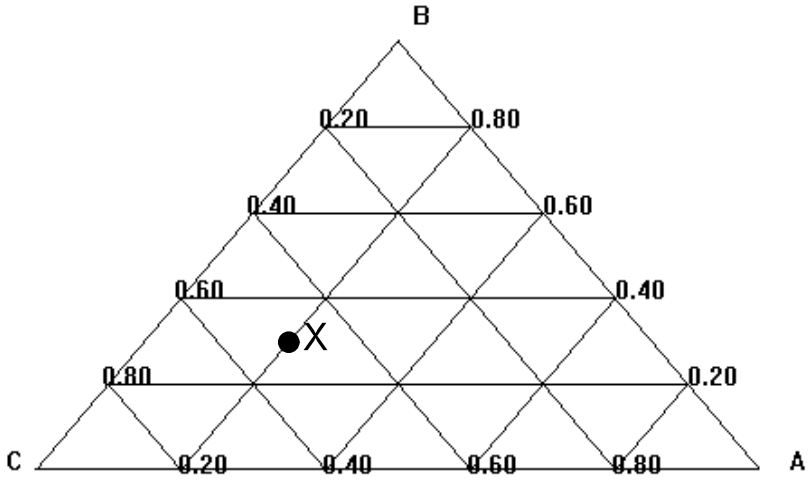

Figure 12: Ternary diagram

By definition any vertex has a coordinate of 1.0 of its respective component. As one moves further from a vertex, the contribution of the vertex component decreases and others increase. In Fig. 13, the point labeled X has composition (A,B,C) = (0.2,0.3,0.5). The tetrahedron is an extension of the ternary diagram to four components, where each face is actually a ternary diagram. See Figure 13 below for an example of tetrahedral coordinates.

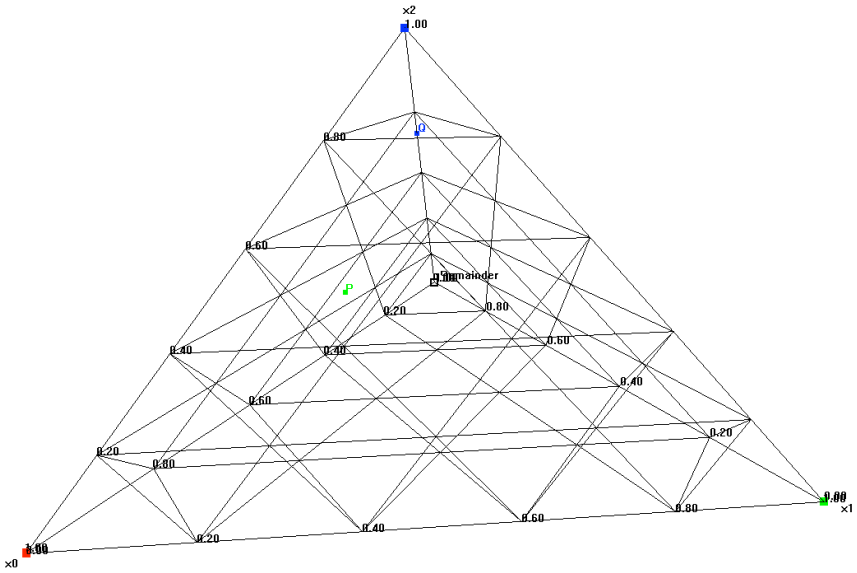

Figure 13. Tetrahedral coordinates

To project higher numbers of components down to the four available, three components are plotted respectively on three of the pyramid's vertices, and there is a choice about the fourth. It can either be the remainder (all of the rest added up), or it can be an individual fourth component. In either case, the totals are always normalized so that they add to 1.

2.3.7 **Dimensionality**

Before visualizing high dimensional spaces, some background about higher dimensional geometry is needed to avoid confusion later. The problem space for the AR visualization is n-d, where n is the number of components in the chemical system. This poses no problem in a theoretical or purely numerical sense, but the trouble is that the AR method is graphical, and it is not natural for humans, living in a 3-d world, to graphically comprehend higher dimensions. For example, what types of entities are possible in an n-d world? The following discussion hopefully answers not only that

question, but also forms a coherent framework for visualizing objects in any arbitrary number of dimensions.

First, only 3 different entities are permitted in any world, regardless of dimension:

- Point – a single location in n-d space, $P(x_0,x_1,\ldots x_{n-1})$
- Curve – several points connected together in a path of straight lines; a single line segment is just a curve with only two points
- Surface – a family of several curves

It will be shown later that the boundary of an AR is of concern and not its interior, so solids are not included as a fourth entity, thus simplifying the problem. (A solid would be defined as a closed family of surfaces.) Entities are always finite size, or zero size in the case of points. For example, there are no lines of infinite length as in Euclidean geometry. Also, notice how each more complex item is built recursively from a family of simpler items. Therefore, the complex entity may always be replaced with many simpler ones, if that makes the thought process clearer. For example, the boundary of an AR is a surface or several surfaces, but this may be considered simply as a large collection of n-d points. If one can visualize an n-d point, one can visualize an n-d curve and an n-d surface. One final note: the use of the prefix “hyper”, as it appears in some of the literature (eg. hyper-plane, hyper-surface, etc.) is avoided in this discussion. It is understood that all spaces are n-d, and calling everything “hyper” adds nothing new.

Points, curves, and surfaces also have their own dimensionality that is independent of the of the original concentration problem space. That is, a way is needed to show that a point has no size, a curve has length, and a surface has length and width. Fortunately, there is a convenient method to do this, the *parametric* form. (Thomas and Finney, 1981) Any geometric entity can be defined parametrically as well as conventionally. For example, think of the familiar definition of a 2-d line. y=mx+b (among other forms) is a conventional equation, but a parametric equation can also be

formed: $\mathbf{x} = \mathbf{x}_{start} + t * \mathbf{x}_{dir}$ Here **x** is a vector **x**(x,y), and t is the parameter. The dimensionality of the original space has been separated from the dimensionality of the parametric space. In the above example, **x** could just as well been 3-d, 4-d, or n-d, and the line would still have one parameter, t. In a similar way, a surface depends on two parameters; u and v are commonly used. Thus, the following conventions result.

- Points are parametrically 0-dimensional entities
- Curves are parametrically 1-dimensional entities
- Surfaces are parametrically 2-dimensional entities

Once again, points, curves, and surfaces exist within an n-d concentration space, and the above definitions do not contradict that, as indicated by the qualifier "parametric". Using the above conventions, a surface in n-d is defined as a parametric 2-d collection of curves, which are in turn parametric 1-d collections of n-d points.

2.3.8 **Convex Hulls**

Given a set of points in a space, the convex hull is the smallest convex set containing the points. It is convenient to imagine a convex hull in 3 dimensions, but it is important to realize that convex hulls can theoretically exist in n-dimensions. The bounding faces of the hull are called "facets". In the 3d case, the facets are triangles, but in the general case they are simplices. For reference, background material on simplices can be found in Bell (Bell, 1987) and Murty (Murty, 1983). There are several algorithms for computing convex hulls, such as incremental, gift wrap, divide and conquer, and quick hull. For an overview, the reader may consult Lambert (Lambert, 1998), and Clarkson offers more detail on the incremental algorithm. (Clarkson, 1993) In the following discussion, reference is made both to n-d convex hulls ("full hulls") and 3-d convex hulls ("view-based hulls"). It is important for the reader to note which type of hull is the subject of discussion, as they serve different purposes.

In relation to ARs, there are three uses for convex hulls. First, some AR data-generation algorithms produce interior points inside the AR as well as border points on the boundary of the AR. Keep in mind that researchers producing candidate data points cannot visualize them until after the data are generated and collated into an input data file for the visualizer, by which time their search for candidate points may have produced both boundary and interior points. In ARs only the boundary is of interest, so interior points can be filtered out by generating an n-d convex hull and determining which of the input points are not included in the hull vertices.

Second, a 3-d view-based convex hull can be computed within the visualization and overlaid on the current 3-d view as a way to check the convexity of the attainable region. By drawing the convex hull as a semi-transparent "skin", it can be seen to coincide with the AR. Finally, the third use is to actually draw the AR surfaces *as the 3-d convex hull.* This is not needed when data are neatly organized into curves and surfaces composed of adjacent curves, but becomes necessary when computer simulations generate data in a disorganized fashion and adjacency information is unavailable.

Convex hull algorithms are a study in themselves. For this reason, previous research by Ken Clarkson of Bell Laboratories, Murray Hill, New Jersey is utilized. (Clarkson et al., 1993) Mr. Clarkson generously provides a complete stand-alone open-source application for computing convex hulls in general numbers of dimensions, downloadable from (Clarkson, 2003). Clarkson's algorithm is an incremental one that grows the convex hull one point at a time. The basic data structure for storing the hull is a splay tree. Splay trees are binary trees that maintain an average or amortized cost per operation of O(logN) through a succession of tree node rotations that keep recently accessed nodes near the top of the tree and also maintain a roughly balanced tree structure. (Weiss, 1999)

2.4 **Attainable Regions**

The application domain of this project is attainable regions or ARs, so some background information in chemical reactor design and ARs is necessary before proceeding further. The AR is a tool to solve the general problem of chemical reactor design synthesis, or the problem of determining some combination of different types of chemical reactors to achieve a desired output. In practice, chemical systems are not limited to just one operation or type of reactor. There are three common types of ideal reactors plus mixing, and they can be combined in an infinite number of combinations through series, parallel, bypass, looping, etc., so clearly it is a large problem.

Even if a physical reactor does not operate ideally, it can often be modeled as a combination of ideal operations. For example, in practice not all of the reactants in a batch reactor may combine, but this may be modeled as an ideal reactor with bypass, so that some of the feed bypasses the reactor and continues to the next stage, as shown below.

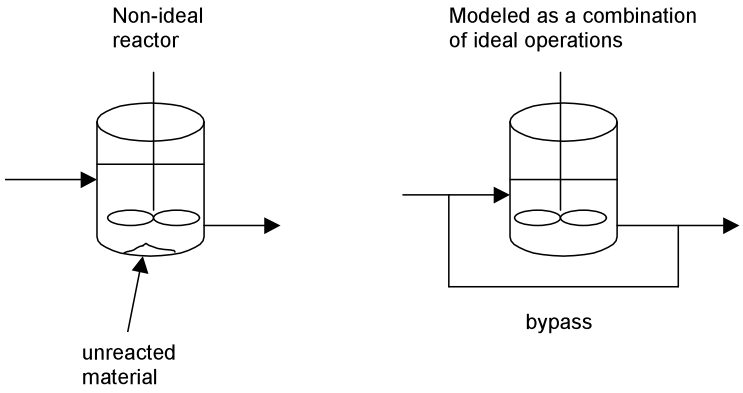

Figure 14. Non-ideal reactor represented using ideal models

To phrase the problem in terms that chemical engineers are accustomed to, chemical plants today are huge, complex, and expensive operations, with thousands of miles of piping such as the Gulf Coast refinery shown below.

Figure 15. Modern chemical plant

The economic stakes are high and trial and error is not a viable approach to building a new system. The object of the AR is to provide the chemical engineer with a theoretical basis for designing a chemical system by graphically enumerating all possible options, without restricting choices in an attempt to keep the problem small. This is contrary to the way that reactor synthesis is often done. For example, without theoretical tools such as the AR, heuristics or “rules of thumb” are often used to limit the problem space. The trouble with this approach is that these decisions may be based more on the way that things have always been done, rather than on science. Not that past experience should be ignored, but new combinations will not be found by relying only on experience and rules of thumb, and there is no guarantee that the optimal approach has not been accidentally ruled out by limiting combinations of operations.

A more scientific method is desired. The first step to finding an optimal system is to determine the space of all possible systems. Then, the optimal or desired solution can be selected from that solution space. The AR is this space of possible combinations, and represents a volume or solid in n-space, where n is the number of chemical components in the system. This first step is of interest in this work, finding the space of all possibilities or AR, and in particular visualizing what that space looks like. The second step, using the AR to identify the desired state and an optimal path to reach that state, can still be a complicated optimization problem and is beyond the scope of this work, but the AR at least defines the possibilities. In the following sections, specific features of the AR are described in more detail.

2.4.1 **Attainable Region Theory**

Attainable regions are not a new idea; Horn first described in 1964 the idea of the set of all possible solutions to chemical reactor synthesis problems, which he called the attainable region. (Horn, 1964) His definition of the AR was quite broad in the sense that he included as variables reactor concentrations, holding time, pressure, temperature, economics, etc. This thesis closely follows the more limited definitions of the AR proposed by later authors such as Glasser, Hildebrandt, and Feinberg, where the AR is restricted to the possible set of reactor concentrations in isothermal reactors involving mixtures of constant density, operating at steady state conditions. (Feinberg and Hildebrandt, 1997; Glasser, et. al., 1987) Four different unit operations are allowed, three of which are types of ideal reactors and the fourth is bulk mixing; all are described in the following sections.

It should be noted that these assumptions are not overly restrictive; many chemical processes are performed using these four operations and under these conditions. Keep in mind that the unit operations can be combined in any conceivable arrangement. On the other hand, processes such as distillation, separation, and other conditions are not included in this work, and perhaps the scope of

future work will be to expand the generality of the method more closely to what Horn originally envisioned.

2.4.2 Terminology and Definitions

Consider the concentration vector at any point in the system as an n-dimensional vector of individual component concentrations $\mathbf{c}(c_0, c_1, c_2,\ldots, c_{n-1})$ where c_i is the concentration of the $(i+1)^{th}$ component of the system in moles per liter. (Vector quantities are denoted with a bold font.) Graphically, the component compositions directly map to coordinates or dimensions in a coordinate system. Let the rate of change of concentration be defined also as a vector, called the rate vector, $\mathbf{r}(\mathbf{c})$, in units of moles reacted per unit volume per unit time. Lastly, define residence time or τ as the time that the reacting material spends inside the reactor; units are typical units of time such as seconds, hours, etc. Finally, concentration and residence time are related, as the concentration within a reactor changes over time, ie., current concentration is a function of residence time, $\mathbf{c} = f(\tau)$.

2.4.3 Fundamental Reactor Types and Operations

Three types of ideal reactors plus bulk mixing are allowed for a total of 4 fundamental operations. The following description is a very brief overview of these operations, but the reader is encouraged to consult a chemical reactor design textbook such as Fogler (Fogler, 1999) for a complete reference. Although attainable regions have been applied to other types of systems such as separations, (Nisoli et. al., 1997) this thesis is limited to the following:

Plug-flow reactor (PFR)

The plug flow reactor, or PFR, is a tubular reactor where the input material enters at one end, flows through the reactor, and exits at the other. In an ideal PFR, velocity is assumed to be in the axial

direction only, and all quantities to be constant in all other directions. The flow is modeled as turbulent plug flow as the name implies, and the PFR is usually diagrammed as shown below.

Figure 16. Plug flow reactor

The PFR is usually modeled by the following differential equation that is integrated along the length of the reactor to determine the concentration at any point along the reactor:

$$d\mathbf{c}/d\tau = \mathbf{r}(\mathbf{c})$$

where **c** is the output concentration vector, **r**(**c**) is the reaction rate vector, and τ is the residence time, which in the PFR is the time it takes one unit of material (eg., one atom) just entering the reactor to make its way to the exit. In an ideal PFR, τ is the same for all atoms of the material at a given position.

Differential side-stream reactor (DSR)

Similar to the PFR, the differential side-stream reactor or DSR is perhaps less common in practice but no less important in theory as it plays a vital role in the AR. Like the PFR, it is a tubular reactor but with additional material being added to the reactor along its length (the side-stream composition). It can be diagrammed as below.

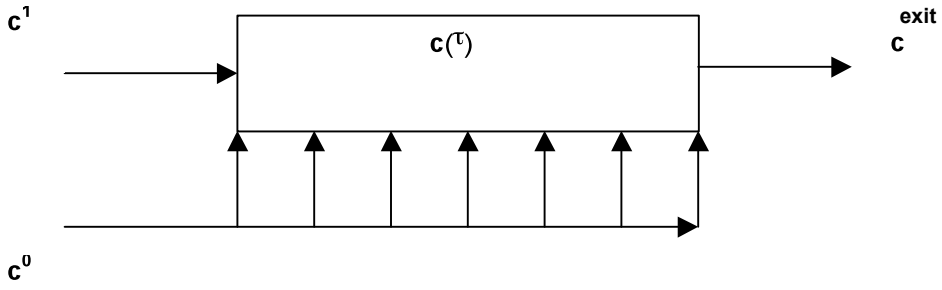

Figure 17. Differential side-stream reactor

$\mathbf{c}^1$ represents the primary feed, and $\mathbf{c}^0$ represents the side-stream feed. The side-stream feed need not be constant along the reactor's length, in fact Feinberg shows that there exists a critical sidestream addition policy for a given DSR. (Feinberg, 1999) This addition policy, so-called the "alpha policy", will be non-uniform but is a function of the position along the length of the reactor. This critical alpha policy is important because it results in the maximum attainable region, but it is also very difficult to compute for higher dimensional concentrations. Feinberg gives the governing equation for a DSR as:

$$d\mathbf{c}/d\tau = \mathbf{r}(\mathbf{c}) + \alpha(\mathbf{c})\,(\mathbf{c}^0 - \mathbf{c})$$

where $\mathbf{c}$ is the concentration vector at some point along the reactor path, $\mathbf{c}^0$ is the side feed concentration vector, and $\alpha(\mathbf{c})$ is the side-stream addition or alpha policy, $\mathbf{r}$ is the reaction rate vector, and τ is the residence time. τ in this case refers to the residence time of a particle from the main input stream, $\mathbf{c}^1$,not the side stream.

Continuous-stirred tank reactor (CSTR)

The continuous stirred tank reactor or CSTR is a reactor type comprised of a large tank that is stirred continuously, so it is assumed that there are no variations in concentration throughout the space of the tank. Therefore, the concentration of the exit material is the same as throughout the interior of the vessel. It can be diagrammed as below:

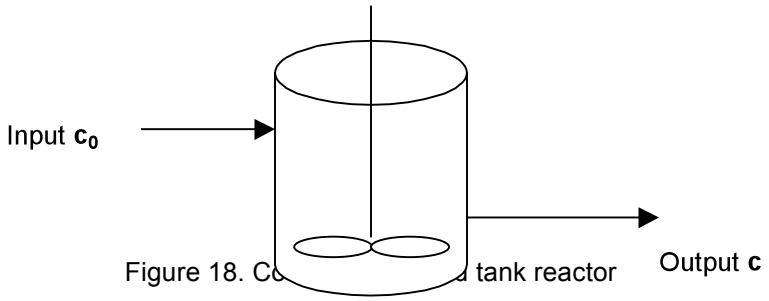

Figure 18. C tank reactor

The ideal CSTR obeys the following algebraic equation:

$$\mathbf{c} - \mathbf{c_o} = \tau\, \mathbf{r}(\mathbf{c})$$

where $\mathbf{c}$ is the output concentration vector, $\mathbf{c_o}$ is the input concentration vector, $\mathbf{r}(\mathbf{c})$ is the reaction rate vector, and τ is the residence time, or the time the material is in the tank. In an ideal CSTR, all atoms of material exiting the reactor have the same τ.

Mixing

Mixing of streams produces intermediary concentrations linearly between two concentration vectors. A bulk mixer allows two liquids to be combined in any convex combination, and it is this operation that gives the attainable region one of its most characteristic properties – convexity. If two points in AR space are attainable, then so are all of the points on the line connecting them.

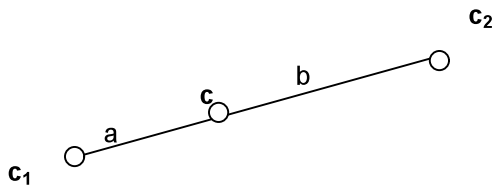

Figure 19. Mixing

$$\mathbf{c} = (b / (a + b))\ \mathbf{c_1} + (a/ (a + b))\ \mathbf{c_2}$$

where **c1** and **c2** are the concentrations at the endpoints, **c** is the resulting concentration anywhere along the line segment connecting **c1** and **c2**, and a is the n-dimensional (n-d) distance from **c1** to **c**, and b is the n-d distance from **c2** to **c**.

2.4.4 **Properties of the Attainable Region**

All of the groundwork is now in place to form an attainable region. The AR is the closed volume in n-dimensional space representing all of the possible (attainable) chemical compositions that can be produced by the chemical system, given some starting feed composition. In evaluating a candidate AR, all of the following test conditions must necessarily hold in order for the AR to be valid. (Feinberg and Hildebrandt, 1997)

- The boundary must be convex, since mixing can fill in any concavity.
- No rate vectors on the boundary may point outward from the AR. They must either be zero, or tangent to the boundary, or point inward. If a rate vector from any point on the AR boundary were to point outward, the AR would have to be extended (grown) because a new, larger AR would be possible.
- No rate vectors in the complement of the AR, when extrapolated backwards, may intercept the AR (known as the complement principle). If such a rate vector were to exist, its base point could be reached from the boundary of the existing AR with a suitable CSTR, again growing the AR.

To summarize, the AR represents the largest possible volume formed by the chemical compositions of the given system, since it represents *all* possible compositions that are attainable. If there is any operation that can make the AR grow larger, then it must grow in order to be valid. The above properties are three ways that this can happen. One final note: the AR represents operations in the theoretical limit. For example, a point may be attainable through an infinitely long PFR. Although in practice this is impossible, it is possible to come arbitrarily close through a sufficiently long PFR.

2.4.5 **Features of the Attainable Region**

Let us now further characterize an AR by the following features, according to Feinberg. (Feinberg and Hildebrandt, 1997)

- The boundary of the AR is a 2d parametric surface, or a collection of such surfaces.
- The boundary determines the AR and vice versa, ie., the boundary is of interest rather than the interior.
- The boundary is divided into surfaces of different types - curved and ruled. The difference is diagrammed in Figure 20 below.

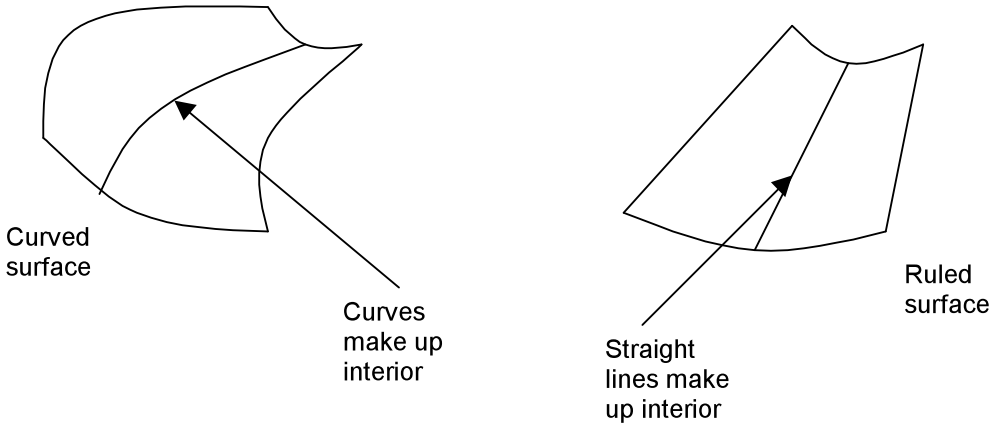

Figure 20. Curved and ruled surfaces

- Curved surfaces correspond to PFR reactors. Feinberg and Hildebrandt call these the "extreme" parts of the surface. All points that are extremes will be found in PFR surfaces, and therefore any extreme point will be reached through union of a PFR trajectory (curve) preceded perhaps by some other type. "PFRs are the highways that provide access to extreme points" (Feinberg and Hildebrandt, 1997)
- Ruled surfaces correspond to mixing operations.
- Junctions between surfaces, called "connectors", are 1-d parametric curves.

- Sharp connectors (adjacent surfaces not tangent) correspond to PFRs (no mixing, only reacting).
- Smooth connectors (adjacent surfaces tangent) correspond to DSRs (mixing and reacting simultaneously).
- Endpoints of DSR connectors (smooth) correspond to CSTRs.

These features are evident in the results of sample problem 1; see Section 4.2. One of the objectives of the AR visualization is to visually verify a candidate AR for validity. Functions built into the program such as pan, zoom, rotate, coordinate system settings, and convex hulls permit the critical viewing of the AR and the ability to quickly and easily spot the above features. When viewing sample problem 1, it is instructive to refer back to this list and look for all of these features in the AR.

2.4.6 **Current Attainable Region Visualizations**

A survey of relatively recent AR literature reveals that visualization in general lags behind other aspects of AR research such as theory, algorithms, numerical methods, etc. The following literature review is not intended to be a criticism of publications in any way. It is however intended to be a justification of the need for better visualization techniques in the AR field. As a direct example of this fact, consider the following correspondence from a collaborator in South Africa. “I am currently developing algorithms for higher AR and have 3D and 4D results. I am struggling with the 4D interpretation, not easy without visualization!” (Seodigeng, 2002, personal communication)

Table I below summarizes eleven AR research papers published in recent years. Current research is focused in a few locations: University of Witwatersrand in Johannesburg, South Africa, Carnegie Mellon University in Pittsburgh Pennsylvania, University of Rochester in Rochester New York, and University of Massachusetts in Amherst Massachusetts. A few trends stand out. First, the most popular visualization method is still the 2-d line graph. Second, another common approach is to discard dimensions altogether from a visualization, usually accompanied by an explanation that only

certain dimensions are of interest. For example, Feinberg and Hildebrandt write: “We shall suppose that A_2 and A_3 are desirable products and that species A_4 has no value.” (Feinberg and Hildebrandt, 1997) Thus, A_4 is not plotted in resulting visualizations and a 4-d problem is displayed in 3-d. Finally, the third approach is to not visualize the results at all in the publication. Even in these cases, a sample problem of a certain dimension is discussed, but results are not displayed graphically.

In the majority of cases tabulated below, the dimensionality of the visualization is less than the dimensionality of the sample problem. This is a contradiction in philosophy to the AR method, which is inherently n-d. The basis for ARs is to display the space of all possible compositions in n-d space. If results are displayed in a reduced space, (for whatever reason) then all possibilities are not visible, reducing the efficacy of the AR method. It must be noted that there is a significant difference between “temporary” dimension reduction on a per view basis, and “permanent” dimension reduction for an entire visualization. The former case is indeed what is utilized in the AR visualization developed for this thesis. A variety of views with different combinations of dimensions can be produced because all dimensions are stored internally and subsets are viewed at any one time. The latter case involves reducing dimensionality from the outset and *only* visualizing certain dimensions. In all of the dimension-reduced visualizations below, no other views of different combinations of dimensions exist, indicating that “permanent” reduction has occurred. One final footnote is that none of the AR literature surveyed utilized tetrahedral coordinates as a display paradigm.

TABLE I

SURVEY OF AR LITERATURE

Paper reference	University	Dimensions of example	Visualized	Dimensionality of visualization	Tetrahedral coordinates	Remarks
Glasser et al., 1992	Witwatersrand	2	yes	2	no	line graphs
Feinberg & Hildebrandt, 1997	Rochester, Witwatersrand	4	yes	3	no	1 variable discarded
Feinberg, 2000	Ohio State	5	no			
Kauchali et al., 2002	Witwatersrand, Carnegie Mellon	4	yes	2	no	line graphs
Hildebrandt et al., 1990	Witwatersrand	4	yes	2	no	line graphs
Glasser et al., 1994	Witwatersrand	3	yes	2	no	line graphs
Godorr et al., 1999	Witwatersrand	4	yes	2	no	2 variables discarded
Smith and Malone, 1997	Massachusetts	3	yes	3	no	good 3d visualization
Nisoli et al., 1997	Massachusetts	3	yes	2	no	line graphs
Balakrishna and Biegler, 1992	Carnegie Mellon	6	yes	2	no	line graphs
Lakshmanan and Biegler, 1996	Carnegie Mellon	6	no			

3. APPLICATION DEVELOPMENT

Many concepts developed in the previous chapter are implemented during the course of developing a working computer application including dimension reduction, various coordinate systems, and convex hulls. Other application features are explored in this chapter for the first time, such as surface rendering, data probing, and development of a standard input file format.

3.1 Introduction

The synthesis of background knowledge from computer science, scientific visualization, and chemical engineering is demonstrated through a working computer program. Two purposes are served by the application development: to gain knowledge and to share knowledge with others. Through collaboration with working researchers in ARs, one goal is to actually help someone else solve a real visualization problem. In this way, not only is knowledge personally gained, but the enhancement of the current state of AR visualization is shared through a scientific community for the benefit of all.

The sections in this chapter may be roughly divided into two categories. The first group, Sections 3.2 through Sections 3.7, describe the implementation of the major contributions of this thesis to the current state of AR visualization and closely relate to the background issues presented in the previous chapter. The second group, Sections 3.8 through Sections 3.11, are a discussion of some of the practical problems that had to be solved in order for the major contributions to become a reality. This group of topics tends to be more specific to computer graphics and somewhat less specific to ARs. It should be noted that while this second group is less theoretical in nature, research was still done into various ways of accomplishing these tasks. This research is documented within these sections rather than separately in the background chapter.

The application is an interactive viewer that allows an AR data file to be read in and viewed in real-time 3d graphics. Choices of coordinate systems (orthogonal and tetrahedral) are available as well as the ability to selectively view 3 or 4 dimensions out of any general number. The program includes interactive viewing controls such as panning, rotating, and zooming, and includes realistic lighting and shading of surfaces. Querying of the data is available through a data probing algorithm; various other controls and options are available such as color choices, labels, etc. Through the use, with permission, of open-source code for computing convex hulls, the program integrates a convex hull computation feature. A data file format was developed for the input of AR data to the program, and is documented in Appendix A. Finally, an “offline” pre-processing utility was written to accept large data sets and filter out extraneous data.

3.2 Platforms

At EVL, there exist a variety of computer graphics and virtual reality hardware and software, including two CAVEs, so some choices had to be made about hardware and software platforms. As can happen, these decisions changed a few times during the course of development. The initial design was to develop a CAVE-based application running under the CAVE Library, on Silicon Graphics machines (IRIX 6.5) and written in C++ and OpenGL. Initial expectations were to gain an advantage in high dimensional visualization through the use of a high-end virtual reality system such as the CAVE. Development proceeded in this direction for several months, then a gradual migration occurred toward a PC Windows-based application.

The reasons are several. From the onset, most of the development was actually done on a Windows laptop running a console-based application that closely resembled the CAVE program. (A console application in Windows terminology is an application that runs in a DOS-like console window, similar to a UNIX console, without any of the Windows GUI features such as menus, dialog boxes, etc.) In this way code was written offline and offsite, and each week ported and tested in the CAVE. This continued for several months, and the user interface primarily consisted of pressing wand buttons in the CAVE. In CAVE terminology, the “wand” is a tracked “3d mouse” with five buttons and a joystick. (Some wand versions have only three buttons and a joystick or trackball.) Navigation is performed by pointing the wand and operating the joystick, and features are selected by pressing the various buttons.

Several ideas slowly evolved. First, testing became more frequent on the Windows console and less frequent in the CAVE, primarily because the laptop could be conveniently set up wherever it was needed, rather than making a trip down to the CAVE, sometimes to find it unavailable, etc. This convenience made it clear that a full-fledged Windows application complete with GUI items such as menus, dialog boxes, and online help would be more accessible than a CAVE program, especially considering that the goal was to collaborate with other researchers who most likely would not have

access to CAVE hardware. Of course, the console application used for initial development had none of those GUI elements, and a good deal of work would be required to build one.

At the same time, the interface elements provided by the CAVE, primarily the wand buttons, became too restrictive. When the program was new and the list of features small, five wand buttons were sufficient, but as features were added the burden on the user became to remember which button or combination of buttons did what. A logical step would have been to display user interface elements within the display space of the CAVE, such as menus and to select menu items by pointing at them with the wand. However, the CAVE system, to the best of our knowledge, does not provide any tools for building standardized user interface elements, as does Windows, or XWindows (the window system under most UNIX operating systems).

That is not to say that GUI elements have not been programmed for the CAVE before; many have been developed during the course of prior work. However, they are all project-specific and not general purpose enough to re-use easily. What is required is a set of GUI building tools such as Microsoft's MFC for Windows, or FLTK for Linux. Recall from Section 2.2.3 that building tools are an essential part of a modern user interface. Without them, all elements would have to be programmed in OpenGL from "scratch". Anyone who has ever done this knows that it rapidly becomes a project in itself, quickly consuming the majority of the application's code. While user interface design is certainly a part of this thesis, it is not intended to become the focus of the work.

The last reason for the switch to a PC application is the growing trend to find economical graphics cards on PCs that rival or surpass the highest-end graphics machines of just a few years ago. Spurred by the computer games industry, high-speed realistic computer graphics can be found on just about any commodity PC, or upgraded for a hundred dollars or so. In general, even at our own EVL lab, the trend seems to be moving toward PCs and PC clusters, both Windows and Linux, and the Silicon Graphics dedicated graphics machines tend to be used less and less.

That is not to say that a PC is the only intended platform for the AR visualization. Future plans are to utilize a tiled display, either monoscopic (2-d) or auto-stereo (3-d) to display results. Recall from Sections 2.1.2 and 2.1.3, that both of these devices provide wide field of view and high resolution, making them primary candidates for this type of scientific visualization. Another advantage is the fact that the tiled nature of the displays lends itself to showing multiple views simultaneously, one per tile if desired. The program architecture described in the following section is designed to be scalable to multiple views. The final advantage that both of these systems have over the CAVE is the availability of a master display, keyboard, and mouse nearby to the tiled display which can function as a “control panel” over the application. On the other hand, in a CAVE setup, this workstation is outside of the CAVE and the user has to remove VR hardware and exit the CAVE to access it.

3.3 N-Dimensional Architecture

The AR visualization internally is an n-dimensional architecture. Hence, it is not restricted to a certain size of problem and can produce any combination of dimensions for a given view. The ability retain n dimensions and change views easily along with interactive graphics features (pan, zoom, rotate, data probing) give it a distinct advantage over generic graphing packages or spreadsheet programs. Although at this time a single view is produced at a time, multiple simultaneous views were a design goal from the start, and the architecture is scalable to readily accommodate this.

Two ingredients are required by an n-dimensional architecture. Data storage must be allocated dynamically and n-d data must be de-coupled from rendered entities. The first item is accomplished by a 2-dimensional linked list. ("a list of lists") For example, imagine a vertically oriented dynamic linked list of points. Since the number of points is unknown, dynamic allocation allows the list to grow vertically. Then, each point can have n-dimensions, represented by the horizontal direction. Each coordinate is a node in a horizontal linked list, as shown in the figure below. Dynamically allocated arrays could have also been used for the same purpose.

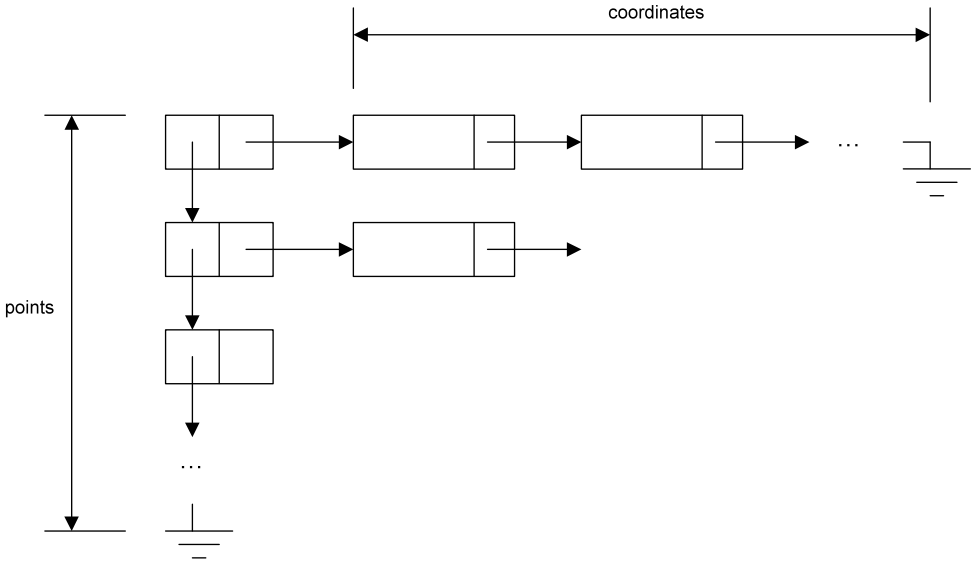

Figure 21. Data structure for storing n-d points

De-coupling of internal data from the viewed display is accomplished using the Model View Controller (MVC) paradigm. MVC was originally developed for programming GUIs to manage user input, output, and internal state and control information in an organized way. (Goldberg, 1984) A key idea of MVC is the separation of the system's model from the user's view of it. Figure 22 below left shows the classic MVC organization. The key point is that even when there are multiple views, there is still only one model, which is view independent. Figure 22 below right shows the situation when there are 2 different views of the same model.

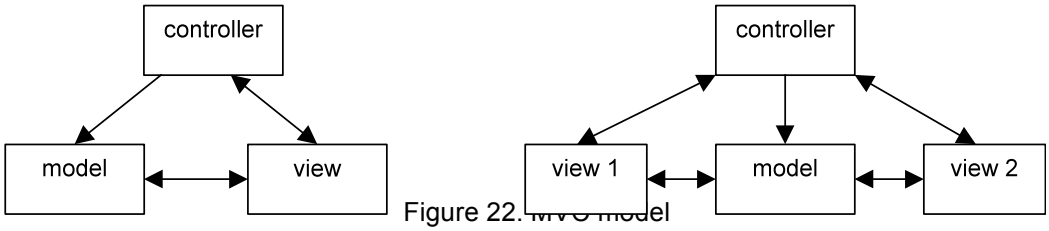

Figure 22. MVC model

The AR visualization architecture closely parallels MVC; the model is the full n-d data, and a view is an individual projection or section based on the coordinate system properties. The controller is just the application. Object-oriented programming encapsulates data structures and methods for each object (class), and makes access possible only through well-defined interfaces. Figure 23 below depicts the structure of the application data class and render class; note the similarity with Figure 22 above.

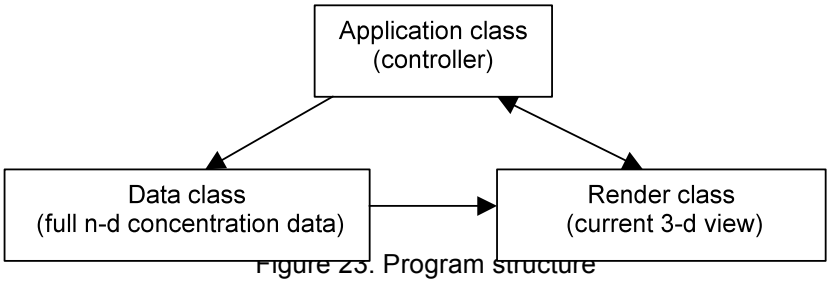

Figure 23. Program structure

3.4 **Data File Format**

The AR visualization is used to see a pre-computed attainable region, and verify its properties and validity. Therefore, the approach is a collaborative one between AR researchers producing simulation data and perhaps other individuals viewing the visualization, as diagrammed below. The focus of this work is on the visualization and AR experts are relied on to provide simulation data, which may occur in a remote location. Moreover, visualization does not have to occur in only one location. Data should be transferable to several locations so that various researchers can view the same results, discuss conclusions and share ideas.

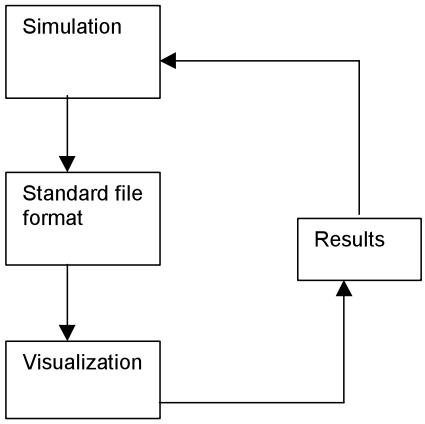

Figure 24. Collaborative approach to visualization

In order for the above scenario to function, there must exist some common format for the simulation output and the visualization input, hence the file format. File names end in the suffix ".ard" (attainable region data) to indicate adherence to the format, but at a low level are simply ASCII text files such as ".txt" files under Windows. The file is organized as follows. A header section defines the file version number, number of dimensions, and names of the components. The next section defines all points of special interest. This is followed by all curves, and lastly by surfaces. Colors can be defined anywhere in the file and changed as often as desired. Labels and a visibility flag may be assigned to any entity. Comments may also be used. The complete format is documented via a sample file in Appendix A and is a significant standardization step for the transfer of AR data.

The format is relatively new (version 1.0) and is still subject to revision through ongoing research. Hopefully one day it may evolve into a standard that all AR simulation programs will write to. As a courtesy to other researchers, outside data was temporarily accepted in any format (eg. multiple smaller files of columnar spreadsheet data) and then parsed and collected it into one ".ard" file. This was done by a combination of text editing and writing small utility parsing programs to help create the final data file. It is expected that in the future AR researchers will perform this process locally, collating their data into a file according to the standard.

3.5 Tetrahedral Coordinates

The tetrahedral coordinate system was introduced in Section 2.3.6 as an extension to a familiar graphing paradigm for chemical engineers, the ternary diagram. Through the use of tetrahedral coordinates, a fourth variable can be displayed in the same view, resulting in a 4-d normalized display. Moreover, the fourth dimension does not have to represent a single component. The first three vertices of the tetrahedron represent individual chemical components, but the fourth, called the "remainder" can selectively represent a single component or some combination of the remaining components. Using the tetrahedral coordinate system together with a remainder axis representing all other components results in a truly n-dimensional display, where all dimensions are viewed simultaneously. This capability represents a significant addition to the current state of high-d AR visualization, and is shown in the example below where all 4 dimensions of a 4-d problem are visible.

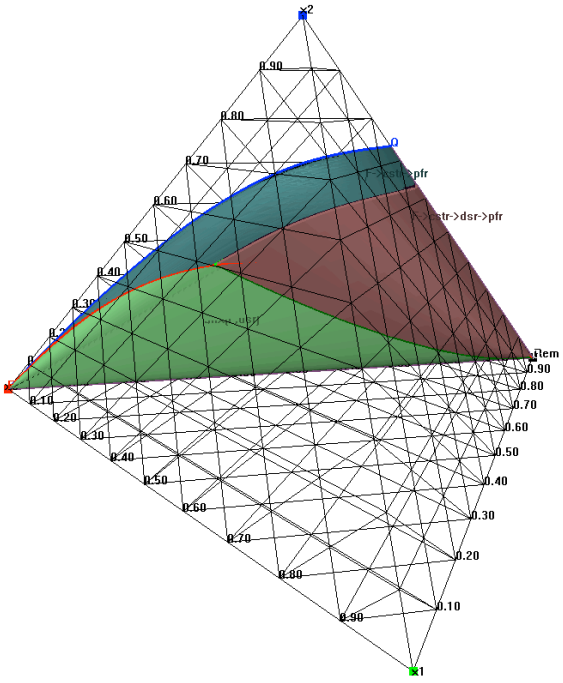

Figure 25. 4-d tetrahedral view

3.6 Dimension Reduction

Along with the tetrahedral system, a conventional orthogonal coordinate system is still available. When using orthogonal coordinates, a subset of 3 dimensions are viewed at a time using dimension reduction techniques as explained in Section 2.3.5 earlier. It will be possible in the future to combine several components into one axis, similar to the remainder axis in the tetrahedral system, but presently only one component is plotted on each orthogonal axis. It will also be possible in the future to plot in orthogonal coordinates with mole fractions, either normalized or un-normalized, although presently concentrations only are plotted in orthogonal coordinates. Dimension reduction methods in orthogonal coordinates are best explained with the help of the user interface for coordinate system properties.

3.6.1 User Interface

The following example is for a hypothetical eight-dimensional system with components named x0 through x7. (The component names are specified in the data file and can be whatever the user desires, eg., chemical formulas, names, etc.) Upon reading in a data file and selecting the coordinate system properties menu entry, the dialog box shown below appears. The default settings are composition using orthogonal coordinates, with the first three components plotted on the x, y, and z axes respectively.

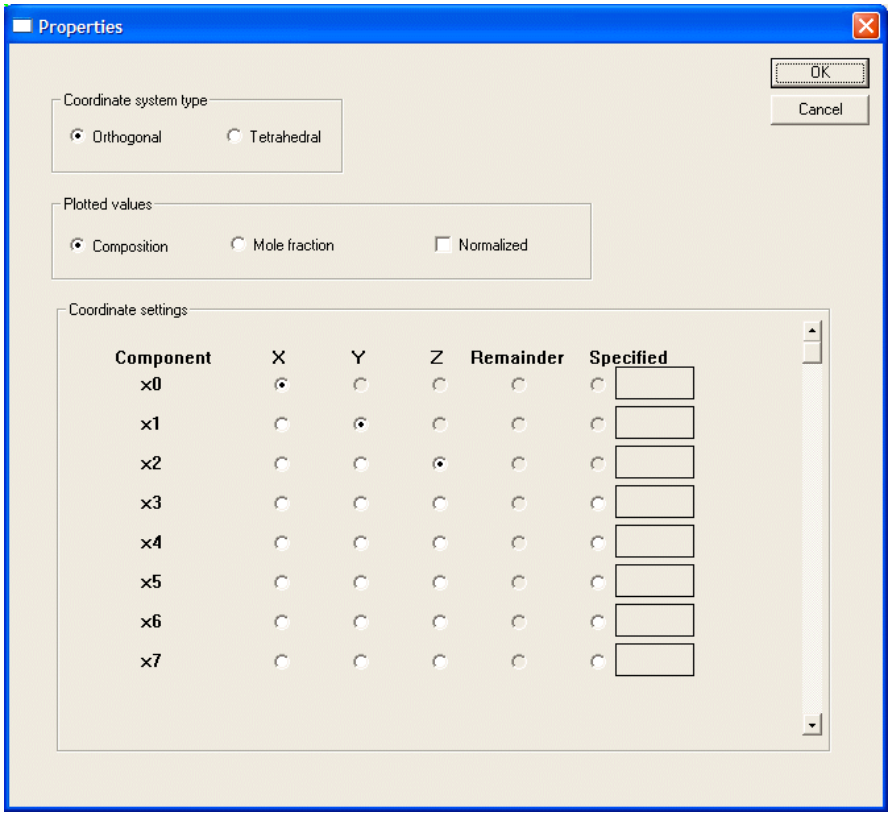

Figure 26. Coordinate system properties

At the top of the dialog box, the first group of buttons controls the coordinate system type. The next group of buttons is used to select composition or mole fraction as the plotted unit. Composition is the concentration of each component, as given in the input data file in a suitable unit such as moles per liter. Mole fraction is an option where the plotted values are the proportion of the component with respect to the whole. When using mole fractions, the entire mixture has a value of 1.0; at any point every component has some value between 0.0 and 1.0 and the sum of all of the components is 1.0. The choice of concentration or mole fraction is available only when using orthogonal coordinates; tetrahedral coordinates are always plotted as mole fractions, by definition.

The lower section of the dialog box is used to set which components should be plotted on which axes, which is the actual dimension reduction part of the interface. The user selects a component to

plot on each of the X,Y,and Z axes. Corresponding radio buttons automatically are enabled / disabled based on prior inputs to prevent the user from composing an invalid view setting. The “Specified” column is used when sectioning instead of projection is the method of dimension reduction, and a cutting plane is specified by fixing the values of all other coordinates except those being plotted. This feature is not yet available, as its need has yet to be determined. Thus far, the projection paradigm has sufficed for the sample problems tested.

To reiterate, in the near future it will be permissible to assign multiple components to any axis in both orthogonal and tetrahedral coordinates, as is presently available for the tetrahedral remainder axis. In this way the user will have complete control over which dimensions to reduce, if any.

3.6.2 **Relationship to Attainable Region Properties**

Recall from Section 2.4.4, that an AR must be convex and that no rate vectors may point outward from the region. If the AR had concavities, they would be filled by mixing, and if the region could have grown outward through outward pointing rate vectors, it would have done so and have been larger. In the simplest terms, the AR must be as large and as full as possible.

In order for visualization strategies such as dimension reduction to be valid, they must preserve the convexity and zero-growth properties of the AR. The effects on convexity and zero-growth of coordinate system choice and dimension reduction are examined next. These are not intended to be rigorous mathematical proofs, but rather intuitive arguments.

First, consider the zero-growth property. This is really a characteristic of the underlying chemical system and is unaffected by the visualization. No changes to visualization properties can change the underlying chemistry governing the problem. As an analogy, consider a three-dimensional volume,

such as a balloon filled with air. Projecting the solid into any 2-dimensional plane or sectioning it with any plane will not change the solid's underlying growth characteristics. Granted, the sections or projections will have different sizes and shapes, depending on the plane, but the boundary is still closed and cannot grow on its own without some underlying physical or chemical change, such as more air being added to the balloon. The choice of visualization can not change the underlying science.

Next one must examine how convexity is affected by dimension reduction, both by sectioning and projecting. In the case of sectioning, convexity is preserved because the section is a subset of the full shape. A subset of a convex shape is still convex. Projecting does not maintain a one-to-one mapping of original points to projected points, as it "flattens" dimensions so that many points in the original data may map to just one point in the projection. The result is that points that used to lie on the convex boundary of the original shape may lie in the interior of the projected shape. This does not pose a problem however, because the boundary of the projected shape will still be convex. The resulting interior points can simply be ignored realizing that they are projections of originally convex points, and only the projected boundary need be checked for convexity. If the original volume was convex, all projections will result in convex boundaries, with perhaps extra interior points.

Convexity under tetrahedral coordinates also must be considered. Tetrahedral coordinates are normalized mole fractions, and this normalizing operation may "shift" points inward, making them appear non-convex. In both sample problems however, all tetrahedral views appeared convex, so it would appear based on this small sample study that convexity may be preserved. Furthermore, normalization is a linear operation, which should preserve convexity. This is an area for further study, hopefully resulting in rigorously-proven theorems. This work thus far provides a starting point for suggested theorems worth further examination.

Convexity needs to be analyzed in the other direction as well. That is, if all projections and sections are convex, the question is whether this is sufficient to show that the original n-d shape is convex. The number of sections is infinite, so examining all section views is impossible, but the number of projections is finite. For example, in a four component system such as sample problem 1, four projections are possible, assuming order of components does not matter. However, checking only the projections is not sufficient to guarantee convexity of the n-d shape. A concavity in the original can occur in what becomes the interior of a projection and be missed. Only by checking all sections, or sufficiently many in a practical sense, can convexity of the original shape be concluded. This may become the definitive reason for requiring that the sectioning paradigm to be completed as another method of dimension reduction.

3.7 Convex Hulls Revisited

In Section 2.3.8, convex hulls were introduced and the distinction between 3-d and n-d hulls was made. Three uses for convex hulls with respect to ARs were listed, and more details about how this is actually done are provided in this section. The convex hull algorithm is used with permission from Ken Clarkson. (Clarkson, 2003) A header comment containing his name, disclaimer, etc. is included in all source files that access his code, per written instructions in that header. His source files, approximately 2000 lines of code, have been included in the AR visualization and modified from a stand-alone application to a function directly invoked from within the application. The generous sharing of his work is deeply appreciated.

3.7.1 View-Based 3-d Convex Hull

A 3-d convex hull is generated to draw a semi-transparent “skin” around the AR, in order to visibly identify concavities or interior points. If the AR is visibly inside of the convex hull in any of the projections, two possibilities exist. Entities may exist inside of the convex hull provided the boundary still coincides with the hull. This is explained in Section 3.6.2 due to the many-to-one mapping of projection. Entities that were on the original n-d convex hull may appear interior in a given projection. Otherwise, if the boundary indeed does not coincide with the convex hull, then the AR is not convex and needs to be extended by adding mixing operations.

Besides using a 3-d hull as an overlay, it may be used as a substitute for surface rendering when existing curves cannot be readily triangulated. In the first sample problem which was computed numerically from a well-known chemical system, curves were listed in the input file in order so that surfaces could be triangulated from them. However, in the second sample problem, curves were listed in no logical order, and there was no knowledge of adjacency or ordering of curves within surfaces. Triangulation would have been difficult at best. The most reasonable and direct solution was to take all

of the points from the curves, and to construct a 3-d convex hull from all of them in any view in order to visualize the attainable region.

To increase execution speed, some minor changes were made to the interface to Ken Clarkson's algorithm. As it appeared originally as a stand-alone program, the routine took its input points either from the keyboard or from an input text file, and sent its output, a list of facets, to either the display or an output file. As a function call within the visualization application, it made more sense to take the input directly from the application's list of rendered vertices, and likewise output the facets directly as a list of to-be-rendered triangles. This saved the overhead of writing input and output files of points and facets.

It was noted earlier that a splay tree is the data structure used by Clarkson. It is an efficient data structure but even so, constructing the view based convex hull in real-time is expensive. The first sample problem contained an input set of roughly 5000 points, and the 3-d convex hull was completed in about 5 seconds. The second sample problem contained an input set of approximately 27,000 points, and took about 15 seconds to run. Tests were performed on a 1.6 GHz Intel Pentium-4 with 256 Mbytes RAM. This operation only needs to be updated when the coordinate system properties change, not upon real-time viewing transformations such as pan, zoom, or rotate, so with an appropriate progress indicator, the application can still be used interactively.

3.7.2 **General n-d Full Convex Hull**

When researchers produce candidate AR data such as in the second sample problem, copious amounts of extraneous data can be produced, and it is useful to reduce the input file size by filtering the data through a pre-processing step. To accompany the visualization application, a pre-processor filtering utility was written. Its input is a ".ard" data file, and the output is a filtered ".ard" data file with extraneous points removed. Points are checked for minimum resolution, and points nearer to each

other in n-d distance than the minimum are removed. Then a full n-d convex hull is constructed based on Clarkson's code, and points not lying in the convex hull are also removed.

The results of the pre-processing can be dramatic. Using a minimum resolution of .001 in the second sample problem, the data size was reduced from approximately 250,000 points to about 27,000, nearly a 10:1 reduction. The operation is an expensive one, $O(n^2)$ because of the minimum resolution check, and the original data set had to partitioned into 5 subsets to be able to run through the pre-processor. Larger file sizes (such as running the entire data set as one large file) could not be handled because of insufficient RAM. Once the program nearly exceeds main memory capacity and begins swapping pages to disk, no further progress is made. However, with appropriate partitioning of the original file into smaller files, each roughly 50,000 point set took about 45 minutes to run on the same 1.6 GHz Pentium-4 with 256 Mbytes RAM. Note that it is valid to partition a convex hull problem into subsets, provided that a final convex hull is found from the resulting sub-hulls.

Aside from filtering out interior points, points are also removed when they are nearer to each other than the pre-set minimum resolution. Data generated by simulations (or computers in general) may be more precise than is necessary. One must consider the final use for the data and then judge how much precision actually makes sense. For example, in the second sample problem input points were supplied in a 16 decimal place format. Considering that most display devices have approximately 1000 pixels in each direction, (eg., 1024 x 768) precision beyond .001 is unnecessary because points closer than that will likely map to the same pixel anyway.

3.8 **Surface Rendering**

A variety of methods exist for constructing a visible surface from a mesh of points, and several approaches were tested for this project. Internally, curved surfaces such as the PFR regions are stored as families of curves of n-d points that are consecutive in residence time, τ. In order to render a surface consisting of several curves, various points are connected by polygons. Triangles are usually used because they are planar and because graphics hardware is often optimized for drawing triangles. Triangulation was chosen for these reasons, but the question is how to go about choosing vertices for each triangle. All of the available points are used, ie., the algorithm never skips any data and never adds any extraneous data. Figure 27 below at left shows a typical strip of triangles between two neighboring curves.

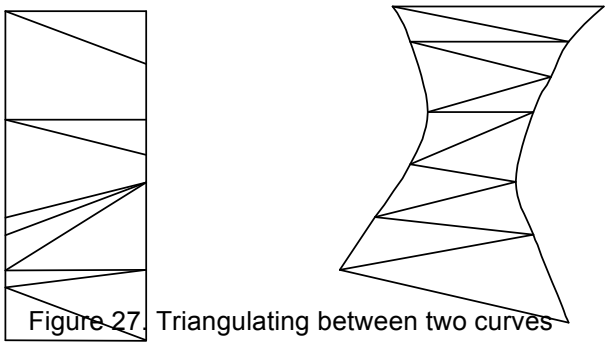

Figure 27. Triangulating between two curves

Note that the trajectories in general will curve arbitrarily in space, and not be parallel or planar. (Each triangle of course is planar.) Figure 27 above right is a more general example. Note also that points along a curve in general are not equally spaced, nor do curves necessarily contain equal numbers of points.

Triangles will approximate the surface most closely when they are fairly regular, and will distort the surface when they become too skewed. In “regular” triangles, edges connect roughly nearby points, and in “skewed” triangles, connecting edges span points far apart on neighboring curves and

approach degeneracy as the points approach co-linearity. Figure 28 below, left and right, shows regular and skewed triangulations, respectively.

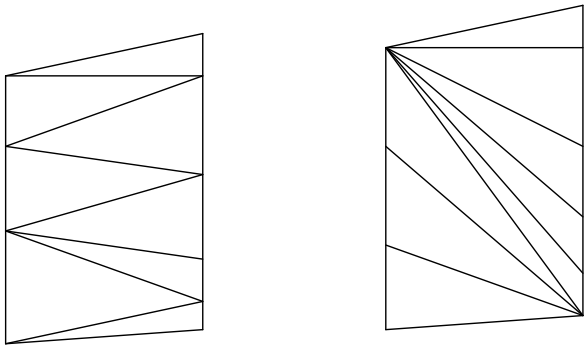

Figure 28. Regular and skewed triangles

Both diagrams use the same data points, but notice how the order in which vertices are chosen affects the quality of the triangles. The right hand diagram results in long, narrow triangles, which will result in a poor surface. The algorithm used for triangulation is as follows: Consider a set of two neighboring curves as above. Starting at the same end of both, connect the end points to form the base of a triangle. Then, consider as possible vertices the next point on either curve. Use a suitable metric to choose one or the other next point as making a better triangle. Connect the diagonal chord which crosses between trajectories, to complete the first triangle. This crossing chord becomes the new base for the next triangle. Repeat the process, always considering as possible vertices the next unused point in each trajectory, and always choose the “better” one. Finally, at the end, one trajectory will be completed and the other may still have some unused points at its end. Form a fan of triangles from the end of the completed trajectory to each unused point in the other.

At each iteration, two candidate points exist, one from each curve, and the question is, what metric should be used to choose the better triangle. A good metric will keep the resulting triangles well-behaved, and a poor metric will skew them more and more. Several unsuccessful metrics were

attempted, among them minimizing the resulting triangle perimeter, minimizing the ratio of the longest to shortest side of the resulting triangle, and minimizing the length of the crossing chord.

Best results were achieved by minimizing the difference of path length fractions along the two trajectories, where the path length fraction is expressed as a fraction of the current path length divided by the total path length. Intuitively, if one trajectory is 10% complete, then the other should also be about 10% complete, where the percentage completed is computed using path lengths (not numbers of data points). Thus, the metric used at each iteration is to choose points that will minimize the difference between path length fractions, where path length is computed in the 3-d projection space. (not the full n-d problem space) Recall from Section 2.3.7 that a path or curve is a 1-d parametric entity, in this case consisting of a set of 3-d points. Triangles are also checked for singularity (collinear points) by testing for zero cross-product of two sides.

The path length fraction works well in all cases seen so far. The figure below shows examples of successful and unsuccessful triangulations from the development of the final algorithm.

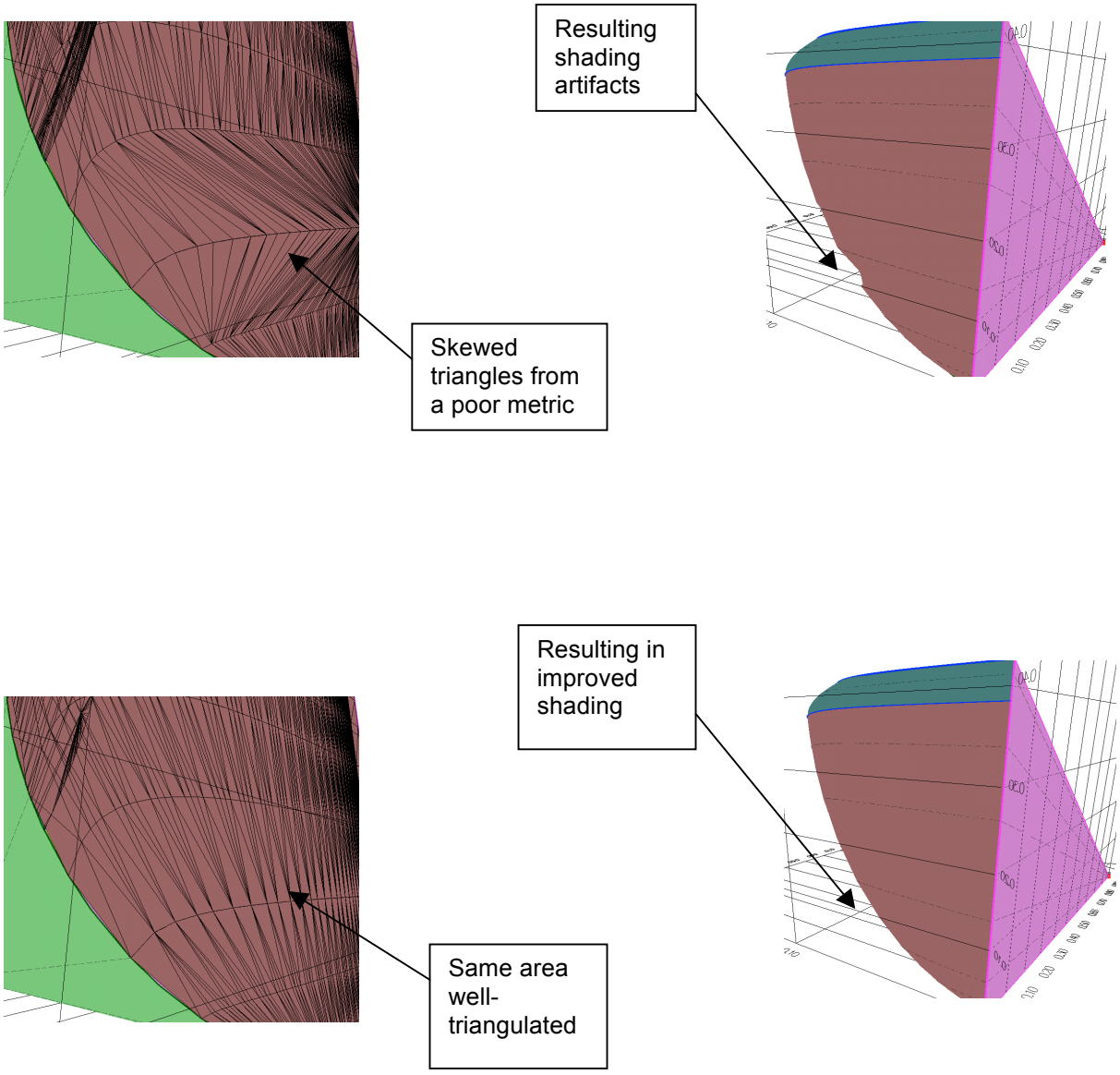

Figure 29. Good and bad triangulations

3.9 Lighting

Lighting can add realism and aids understanding, especially for depth perception. 3-d depth perception is accomplished through 2-d depth cues such as apparent size, perspective convergence, and shading. Without lighting, each rendered surface has its own self-luminous color, but no shadows are cast so the color is uniform across the surface. Other depth cues still help in visualizing the surface, but shading adds a new degree of understandability, albeit at a performance cost. The application originally began without lighting (self-luminous) to maximize performance, but once lighting was added, it was clear that the trade-off was well worth it.

Having said that, lighting is a complex topic with a multitude of possibilities, many of which are not being used here. A simple diffuse white directional light is all that is employed, where the light rays are all parallel as if the source were infinitely far away. Each surface has a defined diffuse material color, so that it reflects the same color diffuse light. Diffuse light is reflected in all directions equally, as opposed to specular light that is reflected in a preferred direction, creating shiny highlights. The light source maintains its relative direction to the viewpoint, shining downward from the viewpoint at all times so that surfaces facing normal to the view appear brightest. A slight amount of ambient light is also added to minimize glare.

A simple lighting model is used not only for performance reasons, but also to avoid distorting or distracting from the data. Tufte stresses the importance of maintaining data integrity and focus on the data, as opposed to obscuring data or replacing it with “pretty pictures”. (Tufte, 1983; Tufte, 1990; Tufte,1997) In keeping with that theme, lighting is used only to help enhance depth perception, but without features such as specularity that would change surface appearance from the basic colors that are defined in the data file. Later, if other visible features such as texture or specularity could be used in a constructive way to represent additional dimensions, then that would justify their use.

As a final note, one drawback of using lighting is that shading is created where it may not be intended. Since surfaces are triangulated, each triangle has a slightly different normal direction than its neighbors, and light falling on these faces gives the surface a more faceted appearance than when it was all the same intensity. Hence, the triangular nature of the surface stands out more, even if the surface should be theoretically smooth. Smooth shading, also known as Gouraud shading, is being used to interpolate the triangle's color between the three respective colors of the vertices. (Woo, et al., 1999) The condition can be further improved by interpolating the normals at each vertex between all of the triangles that share the vertex, as in Phong shading. (Foley et al., 1997) Presently this is not done, as all three of the triangle's vertices have the same normal, that of the triangle's plane.

3.10 Data Probing

Data probing is the opposite of data rendering. Instead of starting with numerical values and producing a rendered image, probing begins with a rendered image and returns numerical values at desired places. The method used is to construct a ray extending from the mouse or wand, and intersect it with all of the visible objects in the current view, as a ray tracer would do. This is done in the order of points first, then curves, and lastly surfaces.

3.10.1 Probing Points and Curves

The first objects to be checked during probing are the "points of special interest." These are the labeled points such as feed point and origin that are identified in the data file. They are relatively few in number, and are not to be confused with the numerous "ordinary" points that comprise curves. Finding whether a point lies on a ray is straightforward; the only problem is that chances are that none of the points lie *exactly* on the ray. However, the point on the ray which is closest to the given point can be found (Glassner, 1998) and then the distance of closest approach is computed. This distance must be less than or equal to some pre-determined probing radius in order to be considered a hit. One final problem is that the probing radius is a floating-point distance in world coordinates, which should vary depending on the current view transformation. To be useful, the probing radius should be equivalent to some small number of pixels in window coordinates (5 pixels, for example, regardless of the current view). Fortunately, the OpenGL UnProject() command (Woo, et al., 1999) can be used to compute this probing radius for any view, based on the number of pixels selected as the margin of probing error. Finally, in case the ray intersects more than one point within the probe radius, the closest point to the viewer is selected.

Curves are handled similarly. All curves are composed of paths of short lines, and probing the curves amounts to finding the intersection of a line with the probe ray. Once again, the chances of two

lines intersecting *exactly* in 3-space are small, but from Glassner (Glassner, 1998) one can compute the respective points of closest approach on the line and the ray, where they are nearest to each other. Again, “hits” are considered to be locations where the distance of closest approach is within the probing radius, and from those curves the closest to the viewer is selected.

3.10.2 **Probing Surfaces**

Since surfaces are rendered as triangles, probing surfaces equates to probing all the visible triangles. The ray usually intersects more than one triangle, in which case the point of intersection nearest to the viewer is the result. The n-dimensional concentrations of that point are then displayed.

Finding the point of intersection of a ray and a triangle consists of several sub-steps, which are outlined in the pseudo-code below (see actual application C++ code, file “probe.cxx” for more details)

a. describe the ray in terms of a parameter t as: ray = base point + t * direction vector
b. construct a plane (ax + by + cz + d = 0) containing the triangle
c. find the point of intersection of the ray with the plane (if it exists) by substituting the ray equation into the plane equation and solving for t
d. determine if the point of intersection of the ray with the plane actually lies within the interior of the triangle

The last step, finding whether a point lies within a triangle given that it lies in the triangle’s plane is actually a sub-problem in itself. Foley and Van Dam (Foley et. al., 1997) give a well-known algorithm for determining whether a point lies in a general polygon, but here a more specific algorithm for triangles is used from Glassner. (Glassner, 1998)

Finally, the result of the data probe is a 3-d point in (x,y,z) coordinates that is a projection of the original n-d data point. The user (eg. chemical engineer) however wants to know the concentrations at

the probed point in terms of the n-d problem space, not the projected view space. The net result is that another step has to occur before the information can be presented to the user: the probed (x,y,z) point in the view space has to be mapped to the original problem space. In theory, the original concentrations or mole fractions can be computed, but the application would have to know the stoichiometry of the chemical system. This information is not stored in the attainable region data file by design because it would be difficult to encode, so the solution is to include a pointer with each vertex in the triangulation to point back to the original concentration problem data.

This provides the n-d concentration at any triangle vertex, but what if the probed point lies in the interior of a triangle, a more likely possibility. The data must be interpolated between the three vertices, based on the location of the probed point as follows. Given the triangle (V0,V1,V2) in Figure 30 and the probed point P, construct a line from any vertex, say V0, through P and intersect it with the opposite side of the triangle to get point A. Linearly interpolate the n-dimensional concentration data from vertices V1 and V2 to get concentration data at point A, and similarly interpolate the concentration data between point A and vertex V0 to get the exact concentration data at the probed point P. If C_i is the n-d concentration at Vi, and | Vi – Vj | is the 3-d distance between Vi and Vj, then:

$$C_A = (C_1 |V_2 – A| + C_2 |A – V1|) / |V1 – V2| \quad (1)$$

$$C_P = (C_0 |A – P| + C_A |P – V0|) / |A – V0| \quad (2)$$

$$C_P = (C_0 |A – P| |V1 – V2| + C_1 |V2 – A| |P – V0| + C_2 |A – V1| |P – V0|) / |A – V0| |V1 – V2| \quad (3)$$

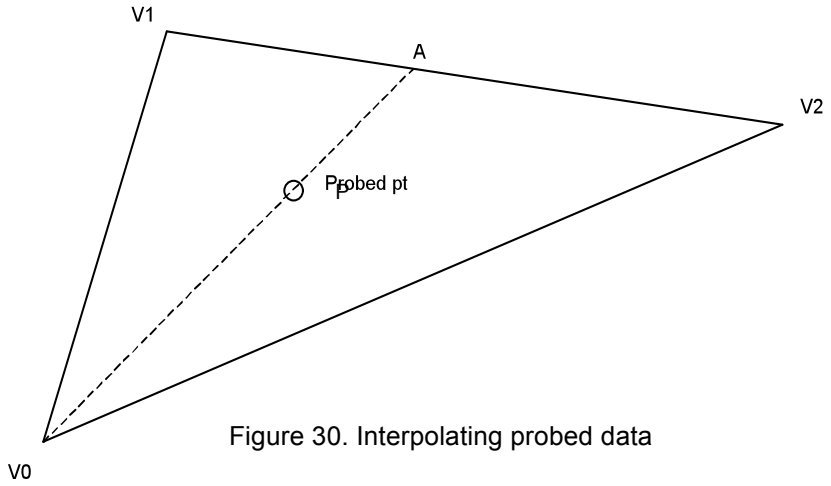

Figure 30. Interpolating probed data

3.10.3 **Labeling**

When probing the visualization, the chemical engineer is asking two questions. What are the coordinates of a desired point, and how (by what combination of chemical processes) can it be attained. The first question is answered by displaying the n-d concentration of the probed point, and the second is answered through the use of labels. Recall that there are four unit operations (CSTR, DSR, PFR, and mixing) which can be combined in any fashion. Since every point on the boundary of the AR is attainable, the question is finding the sequence of unit operations to reach the given point. The sequence is a path along the boundary of the AR beginning at the feed point and terminating at the desired point. This path can follow pre-defined trajectories (eg. the CSTR trajectory) or can lie within surfaces (eg. family of PFR trajectories), can pass through points of special interest, etc.

There is no unique solution for constructing a path along the boundary from one point to another. A reasonable solution may be to follow the most direct route in order to minimize the number of operations, but the exact path choice can still be a complex optimization problem. The scope this work is to display the space of all possibilities, to provide a basis for rational decision making.

Returning to the issue of labeling, various regions of the AR correspond to particular operations. For example, a particular curve may denote a CSTR reactor whose input is the feed concentration, and a particular surface may denote a family of PFR reactors whose inputs are points along the CSTR trajectory. When a probed data point is displayed, its label is shown along with the concentration. Besides labeling probed points, all visible points, curves, and surfaces are identified with leader lines and labels in the view. The labels are stored in the data file format, and technically can be any string. However, labels are intentionally chosen to indicate the type of operation or sequence of operations by which the surface, curve, or point can be achieved. For example, a surface labeled “mix(Q,pfr(F))” indicates that points on this surface can be achieved by mixing a concentration of point Q with the output of a PFR reactor whose input is the feed concentration, point F. Continuing with this example, if point Q is at the end of a curve labeled “F->pfr”, then it can be attained through an infinitely long PFR reactor whose input concentration is the feed. See Figure 31 below.

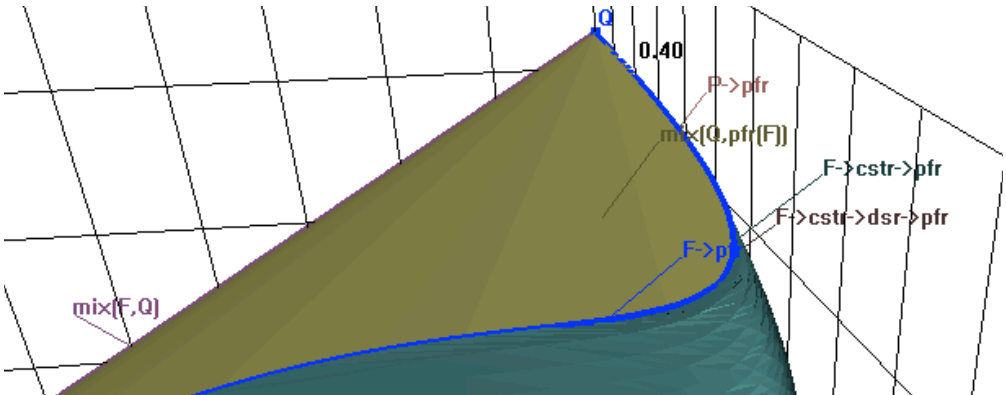

Figure 31. Use of labels

3.11 Grid Scale Values

In any graphing application, even graphing by hand with pencil and paper, the choice of appropriate scale values is critical to a good result. Scale values are minimum, maximum, and either scale step or number of steps for each axis. There are two parts to this problem: providing the user an intelligent way to dynamically adjust scale values, and having the application auto-scale the grid upon initially reading in the data. The dialog box shown below is used to adjust values:

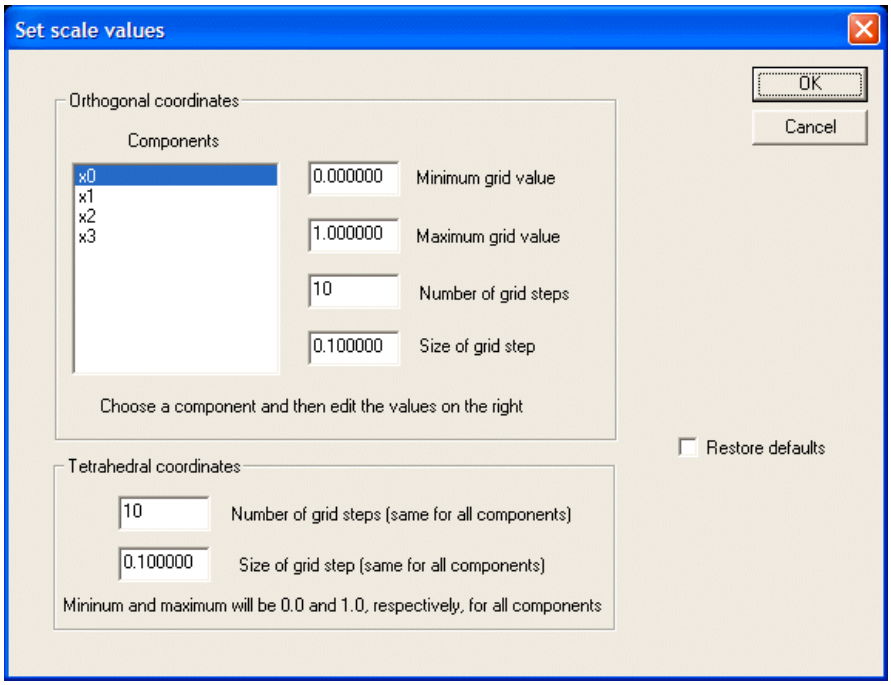

Figure 32. Scale values dialog box

In orthogonal coordinates, the user selects the desired component on the left and then adjusts any of the values on the right. Values that are tied together (such as number of grid steps and size of grid step) are updated automatically when one or the other is changed. In tetrahedral coordinates, all 4 axes have the same scale values, and the minimum and maximum are 0.0 and 1.0 by definition. So the only choice is number of grid steps or size of grid step, which again are tied together. Finally, a "restore defaults" check box serves to return all values to their initial states.

The other aspect of scale values is the determination of the initial defaults upon reading in a new data set. One method initially considered was storing the values within the data file format, although that was rejected because it places the burden on the researcher instead of the application. So, it was decided to program the application to compute scale values automatically. A crude method is to have the program scan the data and find the extents in each axis, and then divide each axis into a suitable number of steps such as 10. While this certainly "works", the results are not always intelligible. When humans graph, we tend to make scale steps "nice" numbers such as powers of ten (.01, .1, 1, 10, …) or perhaps powers of two or five (.2, .5, 2, 5, …). So, after this initial rough computation, the scale step is rounded to the nearest power of 10, 2 or 5, and the minimum and/or maximum are adjusted to be integral powers of that step. For any axis, the following pseudo-code does this:

// find initial step, min and max assumed to be

// extents of data (previously found)

$d_{init} = | max – min | / 10$

// adjust step

$d_{10} = 10 \text{ ^ } (round(\log_{10}(d_{init})))$

if $| d_{init} – 2 * d_{10} | < | d_{init} – d_{10} |$

$d_{final} = d_{10} * 2$

else if $| d_{init} – 5 * d_{10} | < | d_{init} – d_{10} |$

$d_{final} = d_{10} * 5$

else

$d_{final} = d_{10}$

// adjust min, max to be integral amounts of step

$min = floor (min / d_{final}) * d_{final}$

$max = ceil (max / d_{final}) * d_{final}$

4. SAMPLE PROBLEM 1

The first sample problem around which the application was initially designed is a classic in AR literature. J.G. van de Vusse first published this problem in 1964, (van de Vusse, 1964) and the version used here is taken from Feinberg and Hildebrandt. (Feinberg and Hildebrandt, 1997) The chemical system is defined by the following equations.

4.1 Equations and Rate Laws

Chemical equations:

$A_1 \rightarrow A_2$ $\quad k_1 = 1\ [s^{-1}]$

$A_2 \rightarrow A_4$ $\quad k_2 = 1\ [s^{-1}]$

$2A_1 \rightarrow A_3$ $\quad k_3 = 10\ [m^3 / (mol\ s)]$

Let c_i be the concentration of A_i

Feed point: $c_1 = 1.0$, $c_2 = c_3 = c4 = 0.0$

Rate laws:

$$r_{A1} = -r_1 - 2r_3 = -k_1c_1 - 2\ k_3c_1^2 = -c_1 - 20c_1^2 \quad [mol / (m^3\ s)] \qquad (1)$$

$$r_{A2} = r_1 - r_2 = k_1c_1 - k_2c_2 = c_1 - c_2 \qquad (2)$$

$$r_{A3} = r_3 = k_3c_1^2 = 10\ c_1^2 \qquad (3)$$

$$r_{A4} = r_2 = k_2c_2 = c_2 \qquad (4)$$

Through a combination of computations and assistance from a differential equation solver known as Polymath, (Cutlip, 2003) data points were generated for a CSTR trajectory, DSR trajectory, PFR trajectories, and mixing regions. The details of those derivations appear in Appendix D.

4.2 **Results**

The resulting visualization is shown below, in orthogonal coordinates using the projection paradigm with components A_1, A_2, and A_3 plotted on the X,Y, Z axes respectively.

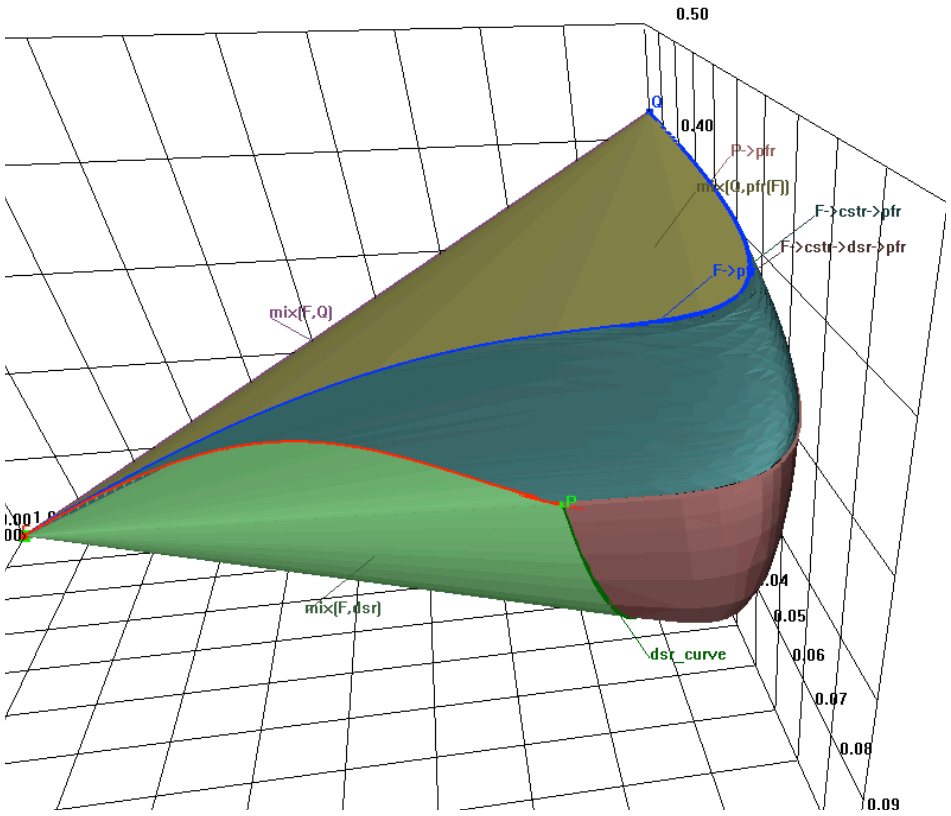

Figure 33. Sample problem 1 results

In (Feinberg and Hildebrandt, 1997) on page 1639, a similar image appears. The differences lie mainly in different scaling factors used for the three axes, making their view appear taller and narrower. However, the coordinates of key points given in the paper are identical to those generated by the application, to four significant digits. The use of labels to identify processes is similar as well,

although Feinberg and Hildebrandt's labels are graphical while the labels generated by the program are text based.

However, unlike a static image in literature, the computer application produces an infinite variety of views through viewing transformations such as panning, zooming, and rotating the view. Moreover, different components may be assigned to various axes, and the system may be viewed in tetrahedral coordinates as well. For example, Figure 34 below shows tetrahedral coordinates with A_2, A_3, and A_4 plotted as X,Y,Z respectively and A_1 plotted as the remainder.

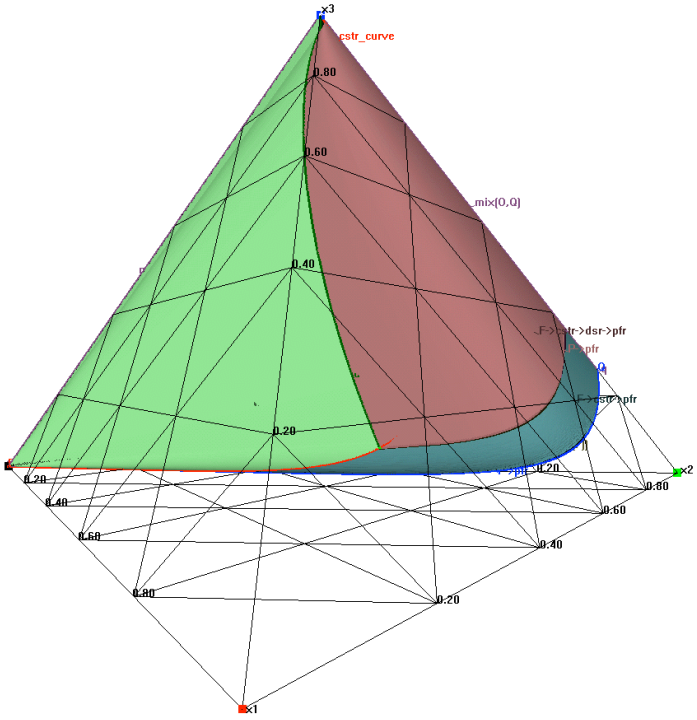

Figure 34. Sample problem 1 tetrahedral view

Features of the AR described in Section 2.4.5 are easily identifiable in the resulting visualization. Ruled mixing surfaces and curved PFR surfaces are present, as well as smooth and sharp connecting

curves. It is instructive to refer back to that section while running the application and note the correspondence between AR theory and practical results.

The van de Vusse problem served as a foundation around which the “core” of the application was developed. Through this problem, many program features were developed and tested, including n-d architecture, dimension reduction, tetrahedral coordinates, standard file format, data probing, interactive viewing, and the user interface. It is a classic AR problem, and the fact the results generated by the application matched other published results was encouraging. The envelope of AR visualization was extended through some of the aforementioned features, but van de Vusse has been visualized many times before using other methods, albeit at the cost of discarding at least one variable. Even our collaborators have such a visualization in Appendix B, generated using MATLAB (MATLAB, 2003). A second, more demanding example was required.

5. SAMPLE PROBLEM 2

Although the Van de Vusse problem is a good first test, a second data set was sought for several reasons. First, higher dimensions were needed to further test the dimension reduction paradigms for both function and comprehension. Second, one of the project goals from the outset was to collaborate with other researchers who are developing AR simulation algorithms that produce high-d results but who are unable to visualize those results. The hope was to combine EVL's visualization expertise with other scientists' AR expertise for the advancement of both disciplines. Lastly, a second data set not created by the program author would serve to further test the application in ways that could not be predicted with locally produced data. Collaboration began early on with the University of the Witwatersrand in Johannesburg, South Africa, because of the AR research conducted by several of the faculty members. (Hildebrandt et al., 1990; Glasser et al., 1994; Godorr et al., 1994) The second sample problem was provided by Tumisang Seodigeng of the Center of Process and Material Synthesis, School of Process and Materials Engineering, University of Witwatersrand. It is a five component system, with components named A,B,C,D,E. Documentation of the data set is included in Appendix B.

Although the researchers' interest is in 4 out of the 5 components, all 5 dimensions are included in the visualization to further test the application and perhaps to provide some results in the fifth component that may prove useful. It is a common strategy to reduce the dimensionality of a problem early on in order to simplify visualization of the results, but this should not be necessary given a good high-d visualization program. The risk of eliminating dimensions that seem unnecessary or irrelevant to the results is that they actually may provide useful information that would never be seen otherwise. So, the approach in this thesis is to store all dimensions, and let the user make dimension reduction decisions later through the use of the program and the generation of visualized views.

One of the features that became necessary through the second sample problem is the convex hull generation; both 3-d view-based convex hulls and full n-d hulls were necessary for the reasons outlined in Sections 3.7 and 2.3.8. Figure 35 shows the visualization without the view-based 3-d hull turned on, and Figure 36 is the same viewpoint with the hull visible. Both figures are shown in tetrahedral coordinates, with components A,B,C assigned respectively to the X,Y,Z axes. D and E together make up the remainder axis.

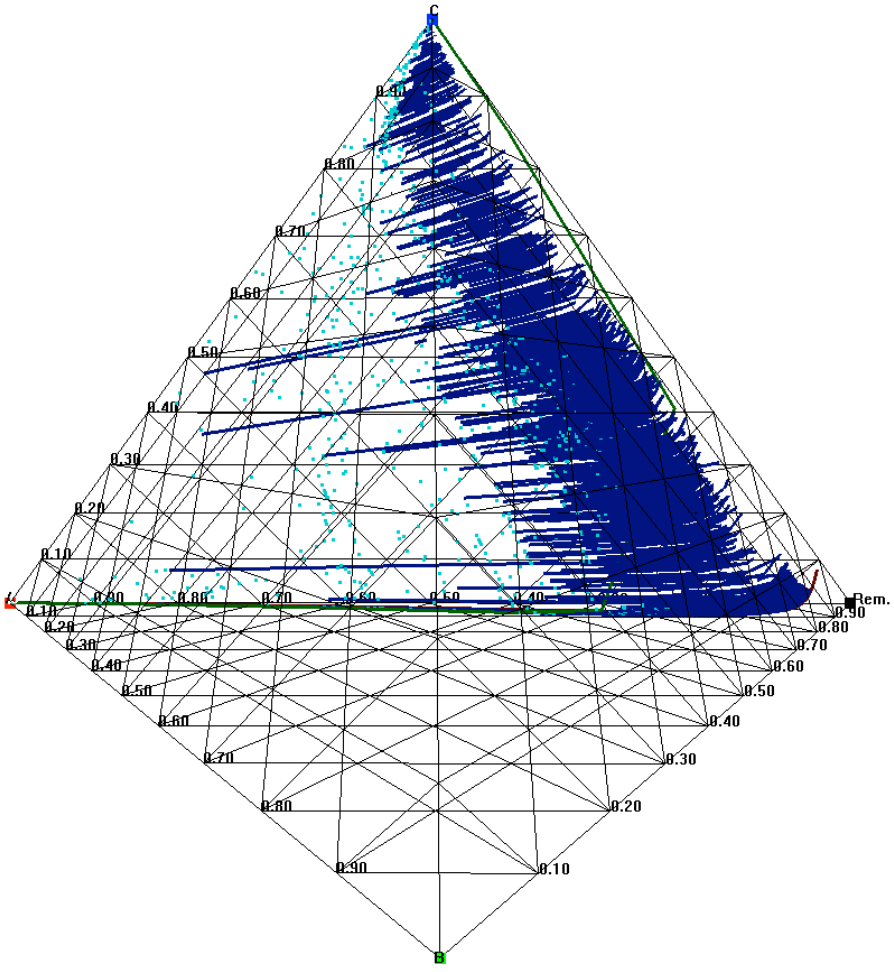

Figure 35. Tetrahedral view of sample problem 2

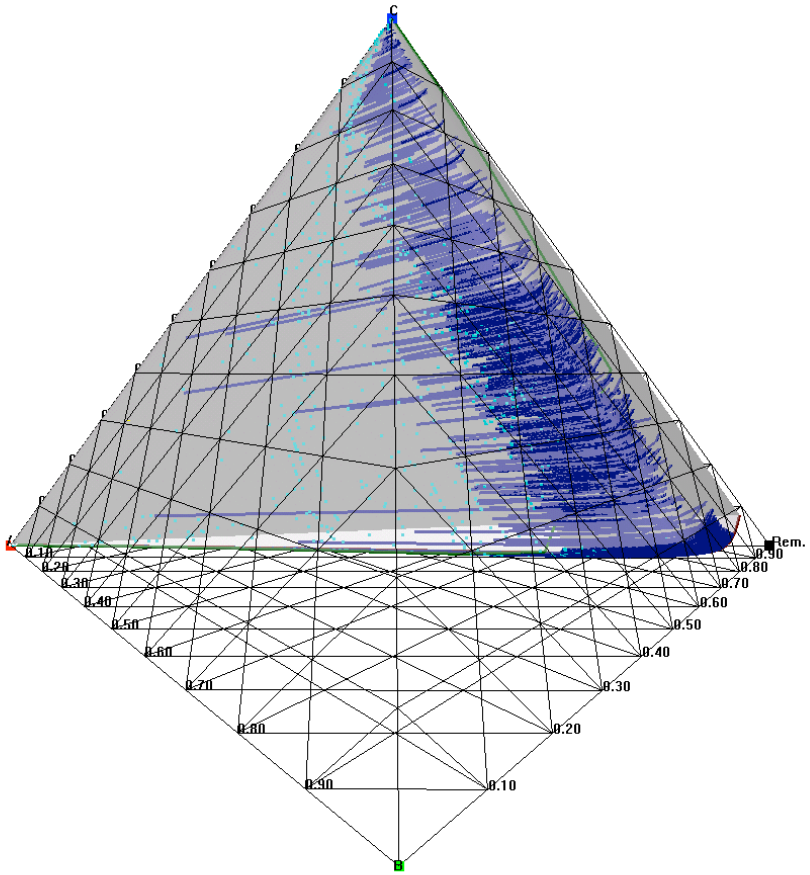

Figure 36. Tetrahedral view with visible convex hull

Characteristics of the chemical system can be spotted at a glance with the AR visualization. For example, notice how little of component E is produced by the system by observing how “flat” the AR is in the tetrahedral view in Figure 37 below. (Component E corresponds to the upper vertex of the pyramid). These are exactly the sorts of patterns that are obvious in a good graphical visualization but difficult to discern in tabular data. Figure 38 is one more screen shot of the second sample problem, this time in orthogonal coordinates plotting components B,C,D with a visible convex hull.

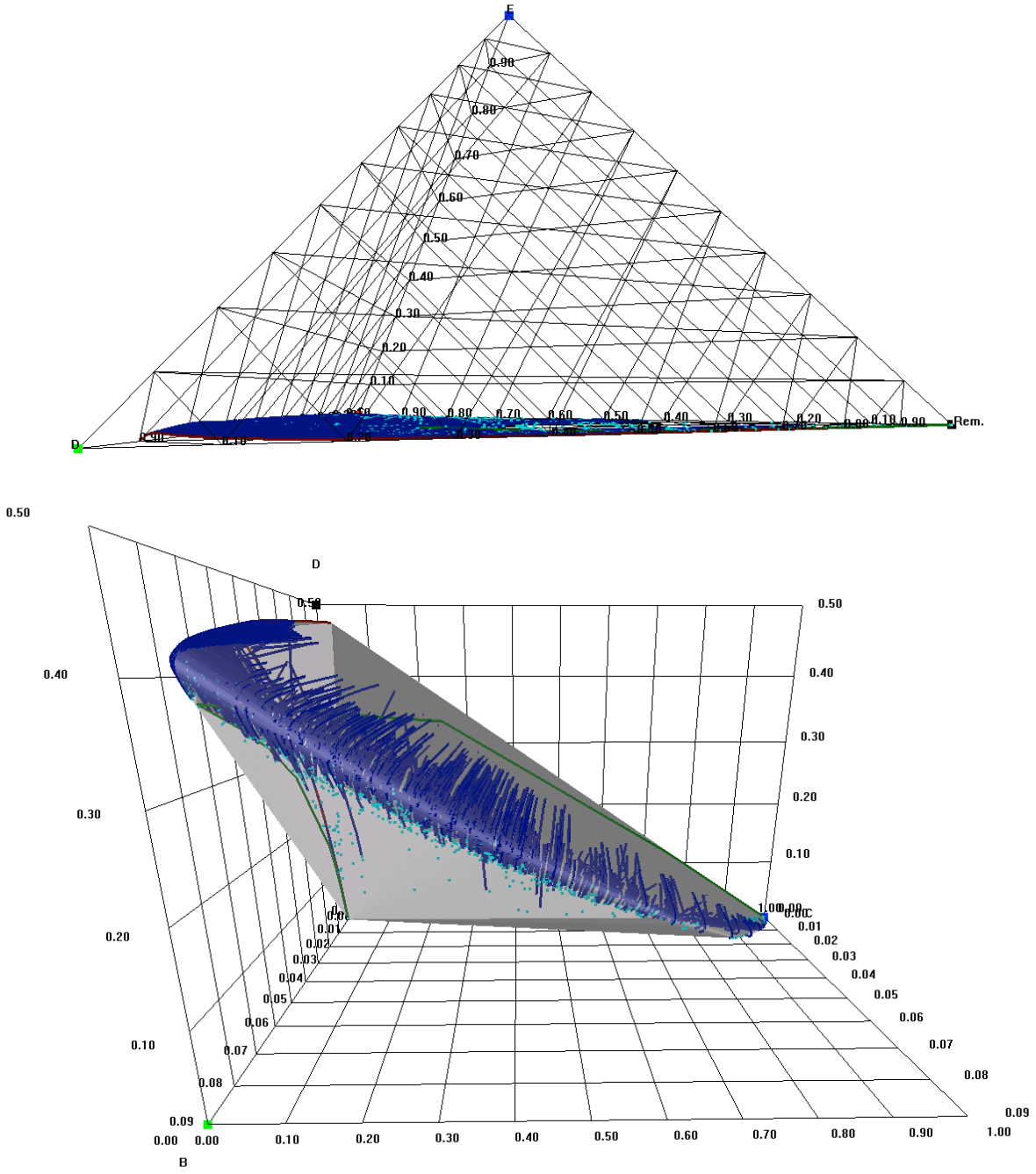

and 3-d convex hulls. It also provided more opportunity for collaboration and testing of the application by other parties. The features developed for the first sample problem together with those added for the second combine to make the application a useful tool for the visualization of high-d ARs. Compared to the survey of visualizations in Section 2.4.6, the ability to view a 5-d problem in 5-d space is a significant step in AR visualization. Our collaborators had no way to previously view these results.

Feedback from Tumisang Seodigeng of the University of Witwatersrand has been positive. The following excerpts are from personal communications via e-mail after sharing results and the program: “Thank you for the program and notes. The first set was very fascinating, I like the idea of switching from one 3D projection to the other with ease (say ABD to ABE) … I have looked at the package Tom sent me some time ago. It was impressive; he managed to sort out the data separation problem.” (Seodigeng, 2003, personal communication) The data separation problem Seodigeng refers to is the fact that points produced by his simulation were disorganized and thus could not be used to render surfaces using triangulation methods, ie., could not be separated into adjacent curves. This was a driving force for inclusion of convex hulls in the application.

One final distinction between the second and first sample problems is data size. The van de Vusse example consisted of roughly 5000 data points, while the second problem consisted of around 270,000 points. This was another factor that necessitated the use of an n-d convex hull in order to pre-process the data set and reduce its size to around 25,000 points, a size that could be viewed interactively on current computer hardware. As ARs grow to higher dimensions and file sizes and data set sizes increase, the techniques developed here can be used to make large data more manageable.

6. CONCLUSION

Background research having been conducted, concepts have been applied to develop a working interactive visualization tool capable of viewing n-d ARs. The application has been tested through two sample problems, and results have been shared with collaborators. This chapter summarizes knowledge gained and plans for future work.

6.1 Summary

Engineering problems that rely on graphical solutions work well in small numbers of dimensions such as 2 or 3, but are difficult to visualize when the dimensional space becomes large. However, scientific and engineering actual problems are multi-dimensional by nature, and graphical visualizations are desired because they leverage the visual perception of the human mind to quickly see patterns and draw conclusions about the data.

One such graphical method in the domain of chemical reactor design synthesis is the attainable region, or AR. The AR is a closed volume in n-d space that represents all possible chemical compositions that can be attained from a chemical system, given some starting feed composition. After research of chemical reactor design synthesis and a thorough survey of AR literature, principles of computer science and scientific visualization were combined to produce a working computer application capable of visualizing n-d ARs. The application program is capable of reading AR data files of the format ".ard" in general numbers of dimensions, and producing views through dimension reduction. Two choices of coordinate systems are available, orthogonal and tetrahedral, along with the capability to view selected combinations of three or four components at a time. A 3-d convex hull feature is included for checking the AR for convexity and for viewing non-ordered surfaces, and n-d convex hulls are also utilized in a pre-processing filtering utility program. Other aspects of the application include data probing, interactive view transformations, grid scale adjustment, color choices, and a functional user interface including a comprehensive help system.

Two sample problems were used to test the application and develop it further. The first problem, the 4-d van de Vusse system is a classic in AR literature. After successfully completing this, a more difficult second test problem was sought. From the outset, one of the goals of this work has also been to collaborate with researchers in the field, because they are the real AR experts. A partnership was formed with the University of Witwatersrand, South Africa, and a second 5-d data set from research currently being conducted was tested. The data was more demanding than the first problem, and forced several new features to be included in the application program. Successful visualizations were shared with the researchers, along with a copy of the application itself. Communication continues between the research parties, and the collaborative effort has benefited all involved. Preliminary feedback from collaborators has been positive. Moreover, a personal visit from Mr. Seodigeng to UIC and EVL is expected later this year, where we expect to meet for the first time in person and discuss findings and future work. The AR collaboration and visualization is expected to continue well beyond the completion of the master's thesis. On a personal note, the opportunity to aid other researchers in their work and the ability to contribute to scientific research in a tangible way has been personally very rewarding.

6.2 **Accomplishments**

The main accomplishments of this thesis can be grouped into two categories: major contributions and other accomplishments. Major contributions enhance the current state of AR visualization. Other accomplishments perhaps do not extend existing work in and of themselves, but were necessary in order to achieve the major contributions and are worthwhile items of knowledge gained. The table below summarizes these categories.

TABLE II

MAJOR CONTRIBUTIONS AND OTHER ACCOMPLISHMENTS

Major Contributions	**Other Accomplishments**
Providing a visualization tool that maintains all dimensions and permits selectively viewing a subset of dimensions under various settings	Interactive features such as viewing transformations (pan, zoom, rotate)
Applying the tetrahedral coordinate system in AR visualization, a useful and familiar display paradigm for chemical engineers	Study of practical methods of triangulating a mesh of points and development of a metric for selecting appropriate points to triangulate
Using n-d and 3-d convex hulls to render disorganized data sets and to filter extraneous data from large data sets prior to viewing	Study of data probing in 3-d space to probe points, curves, and surfaces
Developing a standard file format for the transmission of data sets between simulation programs and the visualization	Functional user interface

6.3 Future Work

As in any research, the work is never complete. After 1-1/2 years and over 7000 lines of code, the project seems to have barely begun. Now that the PC version is complete, which is capable of producing only one view at a time, the next step is to take full advantage of the VR hardware that EVL has available in order to display multiple views simultaneously. Future work to be done includes the following:

- Completing the sectioning paradigm of dimension reduction
- Porting the application to another medium such as a tiled display (Perspectile) or auto-stereo tiled display (Varrier)
- Including simultaneous display of multiple views (appropriate for a tiled display)
- Allowing any combination of components to be displayed on any axis, similar to the function of the tetrahedral remainder axis in the present implementation
- Completing the analysis of convexity properties during projection in the orthogonal and tetrahedral coordinate systems
- Continuing collaboration with researchers to further evaluate the application and determine further needs

CITED LITERATURE

Abbott, E.A.: Flatland A Romance of Many Dimensions. Mineola NY, Dover Publications, 1952.

Achenie, L.E.K., Biegler, L.T.: Algorithmic Synthesis of Chemical Reactor Networks Using Mathematical Programming. Industrial and Engineering Chemistry Research 25 no. 4: 621-627, 1986.

Balakrishna, S., Biegler, L.T.: Constructive Targeting Approaches for the Synthesis of Chemical Reactor Networks. Industrial and Engineering Chemistry Research 31 no. 1: 300-312, 1992.

Bell, J.T.: A Computational Representation of Thermodynamic Surfaces for Use in Process Flowsheet Calculations. Master's thesis, University of Wisconsin – Madison, Madison, WI, 1987.

Clarkson K.L.: A Program for Convex Hulls. http://cm.bell-labs.com/netlib/voronoi/hull.html, 2003.

Clarkson, K.L., Mehlhorn, K., Seidel, R.: Four Results on Randomized Incremental Constructions. Comp. Geom.: Theory and Applications 185-121, 1993.

Cruz-Neira, C.,Sandin, D., DeFanti, T.: Surround-Screen Projection-Based Virtual Reality: The Design and Implementation of the CAVE. Computer Graphics, ACM SIGGRAPH 135-142, 1993.

Cutlip, M.: Polymath Software. http://www.polymath-software.com, 2003.

EVL: www.evl.uic.edu, 2003.

Feinberg, M.: Optimal Reactor Design From a Geometric Viewpoint. Part II. Critical Sidestream Reactors. Chemical Engineering Science 55: 2455-2479, 2000.

Feinberg, M., Hildebrandt, D.: Optimal Reactor Design from a Geometric Viewpoint - I. Universal Properties of the Attainable Region. Chemical Engineering Science 52 no. 10: 1637-1665, 1997.

Fogler, H. Scott.: Elements of Chemical Reaction Engineering 3rd Edition. Englewood Cliffs, NJ, Prentice Hall, 1999.

Foley, James D., Van Dam, Andries, Feiner, Steven K., Hughes, John F.: Computer Graphics Principles and Practice 2nd Edition. Reading, MA, Addison Wesley, 1997.

Glasser, D., Hildebrandt, D., Crowe, C.: A Geometric Approach to Steady Flow Reactors: The Attainable Region and Optimization in Concentration Space. Industrial and Engineering Chemistry Research 26 no. 9: 1803-1810, 1987.

Glasser, B.J., Hildebrandt D., Glasser D.: Optimal Mixing for Exothermic Reversible Reactions. Industrial and Engineering Chemistry Research 31 no. 6: 1541-1549, 1992.

Glasser, D. Hildebrandt, D., Godorr, S.: The Attainable Region for Segregated, Maximum, Mixed, and Other Reactor Models. Industrial and Engineering Chemistry Research 33 no. 5: 1136-1144, 1994.

Glassner, Andrew S.: Graphics Gems. San Diego, Academic Press, 1998.

Godorr, S., Hildebrandt, D., Glasser, D.: The Attainable Region for Systems with Mixing and Multiple-Rate Processes: Finding Optimal Reactor Structures. Chemical Engineering Journal 54: 175-186, 1994.

Goldberg, A.: Smalltalk-80: The Interactive Programming Environment. Reading, MA, Addison-Wesley, 1984.

Hildebrandt, D., Glasser, D., Crowe, C.: Geometry of the Attainable Region Generated by Reaction and Mixing: With and Without Constraints. Industrial and Engineering Chemistry Research 29 no. 1: 49-58, 1990.

Horn, F.: Attainable and Non-Attainable Regions in Chemical Reaction Technique. Third European Symposium on Chemical Reaction Engineering New York, Pergamon Press, 1964.

Johnson, A.: User Interface Design and Programming. http://www.evl.uic.edu/aej/422/index.html, 2002

JuxtaView: http://www.evl.uic.edu/art/template_art_project.php3?indi=242, 2002

Kauchali, S., Rooney, W.C., Biegler, L.T.: Glasser, D. Hildebrandt, D. Linear Programming Formulations for Attainable Region Analysis. Chemical Engineering Science 57: 2015-2028, 2002.

Lakshmanan, A., Biegler, L.T.: Synthesis of Optimal Chemical Reactor Networks. Industrial and Engineering Chemistry Research 35 no. 4: 1344-1353, 1996.

Lambert: Convex Hull Algorithms. http://www.cse.unsw.edu.au/~lambert/java/3d/hull.html, 1998.

MATLAB: www.mathworks.com, 2003.

Murty, Katta G.: Linear Programming. New York, John Wiley & Sons, 1983.

Nielson, G., Hagen, H., Muller, H.: Scientific Visualization. IEEE Computer Society Press, 1997.

Nisoli, A., Malone, M. F., Doherty, M. F.: Attainable Regions for Reaction with Separation. AIChe Journal 43 no. 2: 374-387, 1997.

Norman, D.: The Design of Everyday Things. New York, Doubleday, 1988.

Renambot, L., van der Schaaf, T.: Enabling Tiled Displays for Education. http://www.cs.vu.nl/~renambot/vr/papers/ccviz02.pdf, 2003.

Sandin, D., Margolis, T., Dawe, G., Leigh, J., DeFanti, T.: The Varrier Auto-Stereographic Display. SPIE 4297 no. 25: 2001.

Schneiderman, B.: Designing the User Interface (3rd edition). Reading, MA, Addison Wesley Longman.

Sherman, W., Craig, A.: Understanding Virtual Reality. San Francisco, Morgan Kaufmann Publishers, 2003.

Smith, R. L., Malone, M. F.: Attainable Regions for Polymerization Reaction Systems. Industrial and Engineering Chemistry Research 36 no. 4: 1076-1084, 1997.

Thomas, G.B. Jr.,Finney, R.L.: Calculus and Analytic Geometry. Reading, MA, Addison-Wesley, 1981.

Tufte, E. R.: The Visual Display of Quantitative Information. Cheshire, Connecticut, Graphics Press, 1983.

Tufte, E. R.: Envisioning Information. Cheshire, Connecticut, Graphics Press, 1990.

Tufte, E. R.: Visual Explanations. Cheshire, Connecticut, Graphics Press, 1997.

van de Vusse, J.G.: Plug-Flow Type Reactor vs. Tank Reactor. Chemical Engineering Science 19: 994-997, 1964.

Weiss, M. A.: Data Structures & Algorithm Analysis in C++, 2nd Edition. Reading, MA, Addison Wesley Longman, 1999.

Woo, M., Neider, J., Davis, T., Shreiner, D.: OpenGL Programming Guide. Reading, MA, Addison Wesley Longman, 1999.

APPENDICES

Appendix A: **Data File Format**

The following is a specification for version 1.0 of the AR data file format. The format is detailed by way of a sample valid ".ard" (attainable region data) file:

```
#
#
# File format for attainable region data
#
# author: Tom Peterka
# reviewed by: Dr. John Bell
# date of last revision: 4/7/03
#
# The following is a format for reading / writing n-dimensional attainable region
# geometric data in a text file, which our n-dimensional visualizer will read in
# order to construct the boundary of the attainable region
#



# general notes about the format:


# comments are preceeded with with a pound sign and continue to end of line
# file name ends in .ard (attainable region data)
# blank lines are ignored
# keywords are not case sensitive
# the rest of this document is organized as if it were a sample data file
```

```
# a short header section containing the file version number, the number of dimensions
# and the names of the dimensions in the
# of the problem space must appear first in the file

version 1.0        # version number

dimensions 4          # number of dimensions in concentration space (ie, number of components)
A          # the first dimension in this example is called “A” (can be anything of the user’s choice)
B
C
D

# color may appear any time (optional) and will be effective modally until changed
# default is white or black, depending on background

color 1.0 0.0 0.0    # red color ( r g b format, each color component ranges from 0.0 to 1.0)

# this next section defines points of special interest
# these are not the multitude of points which make up numerous trajectories and
# surfaces, but rather individual points which can be labeled and highlighted in
# the output visualization (eg: the feed point and a few other significant points)

point npoints
# point is the name of this section
# npoints is the number of points in this section
# next will follow ‘npoints’ number of lines of the following format
```

```
a b c d [T/F] [label]

# a b c d are the component concentrations, replace with floating point numbers or scientific notation
# label is optional, and will be displayed next to the point
# [T / F] is a visibility flag, T = draw the object, F= don't draw
# visibility is optional, except when a label is used, visibility is
# mandatory (to enable parsing)

color 0.0 1.0 0.0       # switching to blue color, for example

a b c d [T/F] [label] # labels may have spaces, and extend to the end of line
a b c d  # default visibility is T, no label for this object
...

# this next section defines curves
# curves are used in a general sense to include: a individual point, a line segment
# (2 points), or a trajectory (any number of points)
# curves may be of the following types: mixing line segment, CSTR trajectory,
# DSR trajectory, or PFR trajectory
# note that any of the above curve types may be degenerate and have only one point

mix npoints [T/F] [label]  # mixing line segment, 1 <= npoints <= 2
a b c d
a b c d
mix npoints [T/F] [label]   # each curve individually identified by a new command
a b c d
```

a b c d

cstr npoints [T/F] [label] # CSTR trajectory, npoints >= 1

a b c d

...

dsr npoints [T/F] [label] # DSR trajectory, npoints >= 1

a b c d

...

pfr npoints [T/F] [label] # PFR trajctory, npoints >= 1

a b c d

visibility is used in the same way as above in the point section

label is similar, except that labels are required whenever the curve will be referred to below in a surface

this is typical, so most of the curves will have labels, and these labels are not displayed in the visualization

...

this last section defines surfaces

surfaces are a triangulation of 2 or more of the above curve types

if the number of curves is > 2, then the curves must all be of the same type

if ncurves = 2, then the curve types may the same or different

if different, then the result is a mixing surface between the 2 curves

if ncurves > 2, then the curves must be listed in order (adjacent in the surface)

ie, the surface will be triangulated by taking two adjacent curves at a time

surface ncurves [T/F] [label]

label 1 # label of a curve

label 2 # label of a curve

...

default color for surfaces is the average of constituent curve colors

(specific color can always be given with the color command (recommended))

Appendix B: **Sample Problem 2 Materials**

The following two documents were provided by Tumisang Seodigeng. They are re-printed here for reference as supporting documents for the second sample problem, without any corrections or modification. The entire documents are included, including any fonts, figures, etc. that appeared. Figures are not listed in the table of figures and fonts may not be the same as in the thesis text. No attempts were made to modify any of this data; it is meant to be included as a whole, in its original form. The documents were received as personal communication, not as published or copyrighted material.

B.1 **Initial Documentation of Sample Problem 2 Dataset**

The following is an initial document that accompanied the data set (TP)

The 4D study case

A $k_{1f} \leftrightarrow k_{2r}$ B $k_3 \rightarrow$ C

$\downarrow k_4$ $k_{5f} \updownarrow k_{6r}$

½D E

We are looking at the ABDE space. We built the candidate ARs using the algorithm we call 'DSR Algorithm'.

The DSR algorithm traces out the optimal DSR (Feinberg 2000 ***a*** and ***b***) using constant alpha values. We believe that a DSR in 4D is a surface, (as it is a curve in 3D).

My algorithm constructs 3D ARs successfully. These are the results for a 4D trial. I am working in the ABDE space.

The attached files are

cstr.txt contains cstr loci from feed. Columns are [A B C D E tau]

pfr.txt plug flow trajectory from feed. Columns are [A B C D E tau]

cdsrxtr.txt points on the DSR surface, Columns are [A B C D E tau alpha]

pfrhiways.txt manifolds of pfr trajectories starting from the DSR surface
Columns are [A B C D E tau alpha]

Space.txt all points in the space, (mess!)

Tau – residence time

Alpha – mixing policy value
If negative the point is a CSTR
Zero for a pfr
Any positive value for a DSR

There is also a cdsrxtr.mat file attached which as matlab file containing binary data of the above. Abde4d points on the DSR surface. Others have the same name as above.

Extras are

k - rate constants as in the reaction above

alpha – constant alpha grid

co – feed

B.2 **Follow-Up Document**

Later, a document was received from Mr. Seodigeng clarifying the determination of the alpha policy used in DSR tractories. Recall that alpha refers to the sidestream mixing policy for a differential sidestream reactor, or DSR. This document is re-printed below. Again, it was received as personal communication, not as published copyrighted material. No changes, corrections, or additions were made to it. (TP)

The constant alpha story

The original idea here was to take alpha values from the optimal alpha DSR and integrate them back as constant alpha DSRs (CADSRs) to see they terminate. This idea fell apart because the CADSRs can be tracked back into negative concentration space without showing any trends or whatsoever.

Starting constant alpha DSRs from some extreme points, results in an envelope that closely delineates the optimal DSR. See figure 1. The extreme points where these constant alpha DSRs can start differ from system to system. For a Van de Vusse kinetics, the CSTR equilibrium point is a good starting point for the first optimal DSR. (figure 1).

I have derived some general guidelines on which extreme points to use depending on the system and we are still checking for the generality of these guidelines.

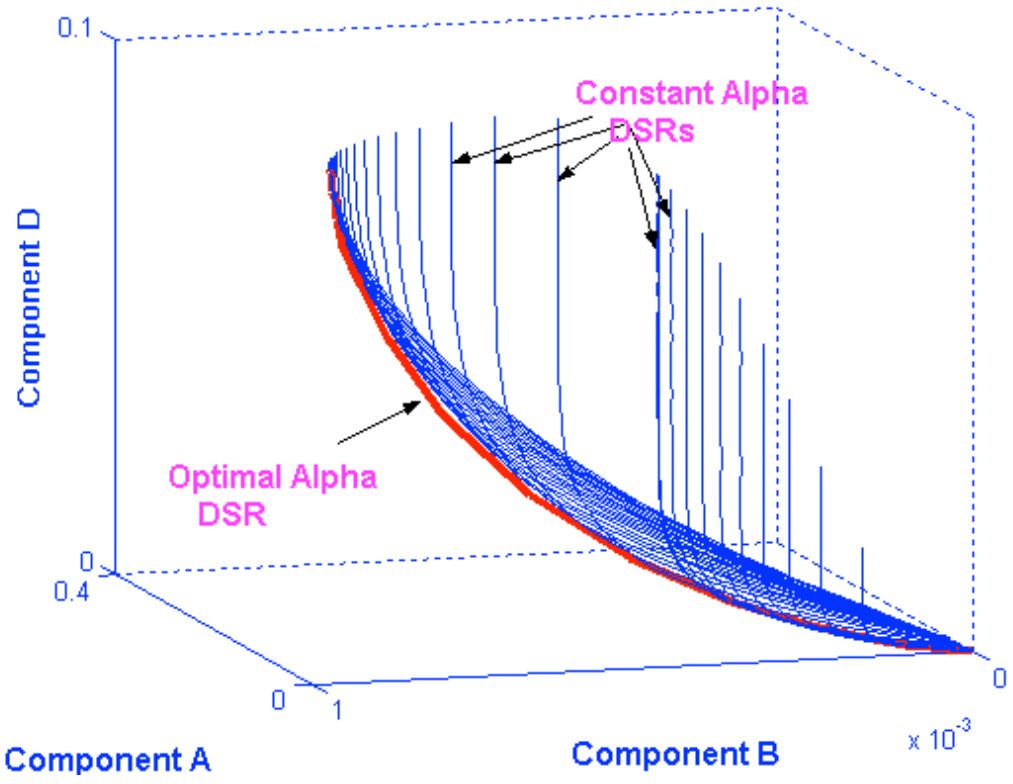

Figure 1.

A few iterations and checking the rate vectors can end up with constant alpha DSRs touching the optimal DSR and falling back into the region.

The cunvhull of the structure shows points from constant alpha DSRs lining along the optimal DSRs (see figure 2). This technique solves candidate ARs and delineates the optimal DSR also showing how alpha changes along the optimal DSR without solving complicated equations. The results agree with Feinberg's optimal DSR.

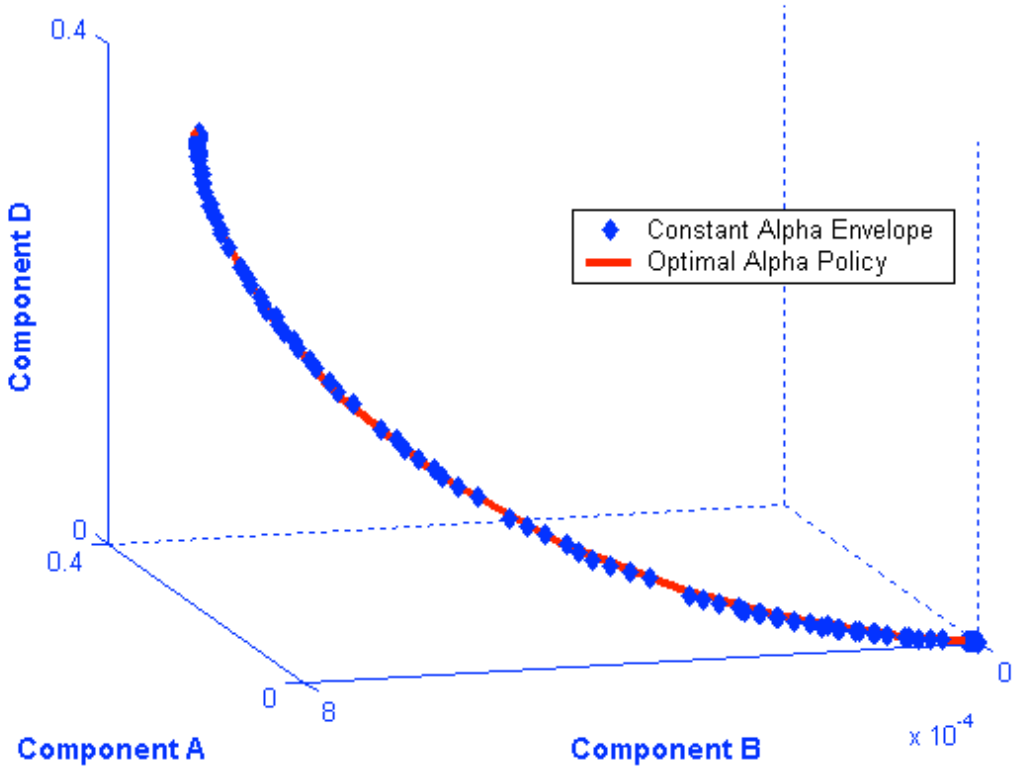

Figure 2

Below is the candidate AR for the Van de Vusse kinetics built using our technique (fig 3)

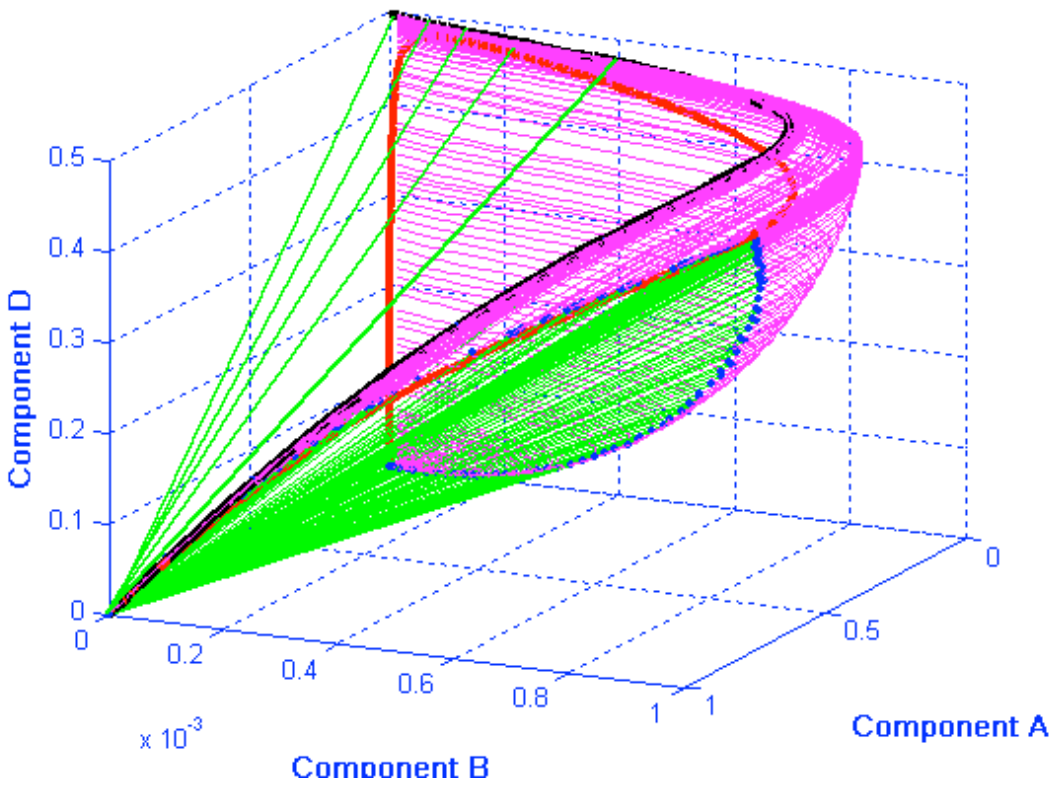

Figure 3

The candidate AR built using Feinberg's optimal policy is shown below

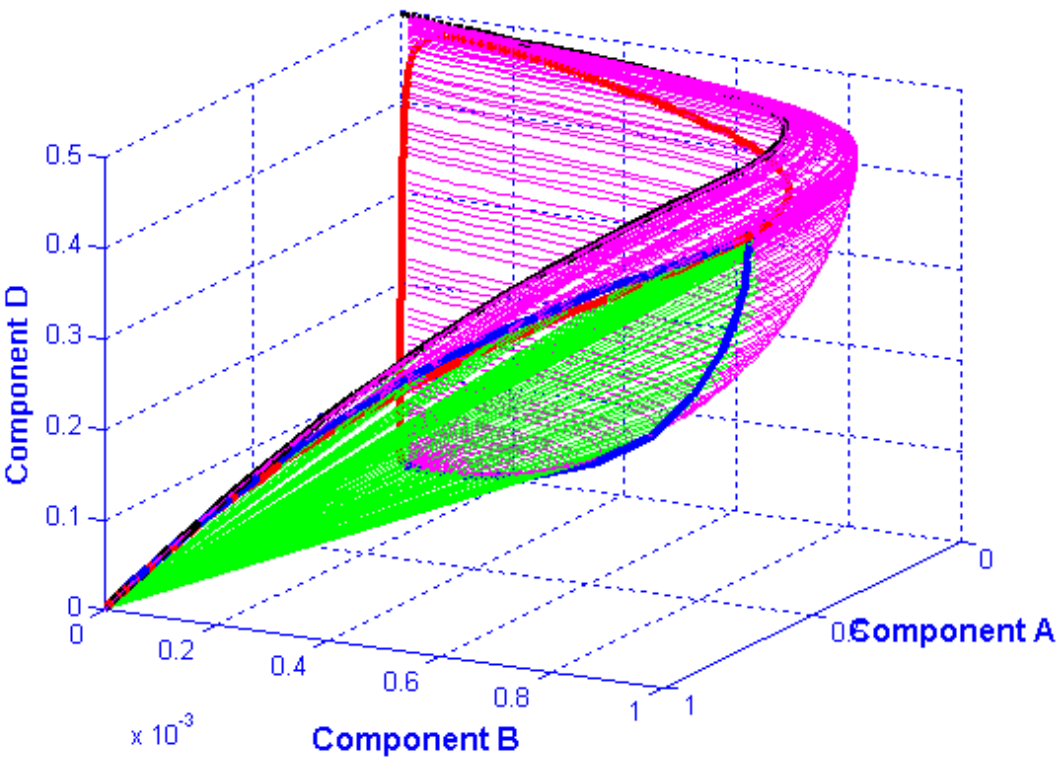

figure 4

I have implemented the algorithm in Matlab and generated the AR in runtime of 40seconds. The algorithm is faster (way faster) than the two previously developed by my co-researchers. More interesting is the generality of the technique and how easily it can be extended to systems with heat and mass transfer.

With this technique I am building candidate ARs for more practical kinetics, for which optimal DSR equation ***cannot*** solved because complicated rate equations. I am currently working on Methane Steam Reforming using modified Xu and Froment kinetics. I hope we will work together on the visualisation of these study cases.

Appendix C: **Evaluation Survey**

The following survey / questionnaire is to be used in the future for user evaluation of the application.

Please circle the best answer to each question. All responses are used strictly for the improvement of the application program and will remain confidential. Thank you for your cooperation.

1. Rate your previous experience in computer operation and software applications in general.

1 2 3 4 5

beginner expert

2. Rate your previous experience with scientific visualization applications.

1 2 3 4 5

beginner expert

3. Rate your background knowledge in the field of attainable regions.

1 2 3 4 5

beginner expert

4. If you used the ".ard" file format to create or modify your own data file prior to reading it into the visualization, please comment on the file format. If not, skip this question.

1 2 3 4 5

difficult easy to use

1 2 3 4 5

too rigid flexible

1 2 3 4 5

confusing clearly documented

5. If you know what processor, processor speed, amount of RAM, or graphics card your system has, please provide any information known to you. If not sure, skip to the next question.

Processor type and speed _____

Amount of memory (RAM) _____

Graphics card and video memory amount _____

6. Rate the performance of the program on your system.

1 2 3 4 5

slow fast

7. Is the layout of menus and toolbar buttons intelligible?

1 2 3 4 5

confusing clear

8. Comment on the usefulness of the online help system.

1 2 3 4 5

useless helpful

9. Rate the features in the scale values dialog box.

1 2 3 4 5

confusing helpful

10. Rate the features in the coordinate system properties dialog box.

1 2 3 4 5

confusing clear

11. Comment on the overall concept of dimension reduction as used in the program. (viewing a subset of dimensions at any one time)

1 2 3 4 5

confusing clear

1 2 3 4 5

limited value valuable

12. In terms of dimension reduction methods, do you think the sectioning method would be helpful or necessary, or is the projection method sufficient. The sectioning method uses the “specified” values in the coordinate system properties dialog box, but is non-functional at this time.

1	2	3
sectioning is needed	not sure	projection is sufficient

13. Rate the interactive panning, zooming, and rotating view controls.

1	2	3	4	5
difficult				easy

14. Did the use of the program help you recognize patterns in your data and draw conclusions about the data?

1	2	3
no	somewhat	yes

15. Comment on the overall goal of the project, which is to make high dimensional attainable region data comprehensible.

1	2	3	4	5
failed				succeeded

16. Rate the usability of the tetrahedral coordinate system

1	2	3	4	5
not helpful				valuable

16. Please feel free to add any additional comments, suggestions, questions, etc. in the space below or on the back:

Appendix D: **Derivation of Sample Problem 1**

The following are the original notes of the derivation of various trajectories and surfaces for the first sample problem.

D.1 CSTR Trajectory

Referring to Fig. 1, p. 1639 of (Feinberg and Hildebrandt, 1997) first plot the CSTR trajectory from point F to point P.

The defining equation of a CSTR is $c - c_o = \tau\, r(c)$, (τ is space-time)

c_1:

$c_1 - c_{10} = \tau\,(-c_1 - 20c_1^2)$, where c_{10} is the initial value of c_1, the feed point, 1

$c_1 - 1 = \tau\,(-c_1 - 20c_1^2)$

$0 = -20\tau c_1^2 - \tau c_1 - c_1 + 1$

$0 = 20\tau c_1^2 + (\tau + 1)c_1 - 1$

from quadratic formula, $c_1 = [\,-(\tau+1) +/- \text{sqrt}(\,(\tau+1)^2 - (4)(20\tau)(-1)\,)\,]/\,[(2)(20)\,\tau]$

since $\tau >= 0$, $-(\tau+1) < 0$, so must use positive root to get $c_1 >= 0$

$c_1 = [\,-(\tau+1) + \text{sqrt}(\,(\tau+1)^2 + 80\tau\,)\,]\;/\;[40\,\tau]$

c_2:

$c_2 - c_{20} = \tau\,(c_1 - c_2)$

$c_2 = \tau c_1 / (1 + \tau)$ (c_1 is already known from above)

c_3:

$c_3 - c_{30} = \tau\,(\,10c_1^2)$

$c_3 = 10\tau c_1^2$

c_4:

$c_4 - c_{40} = \tau\, c_2$

$c_4 = \tau c_2$

In Feinberg and Hildebrandt, point P is (c_1 = .2236, c_2=.0868, c_3=.3172, c_4 = .0552) with τ =.6345 ; this coincides with our results.

D.2 **PFR trajectories from CSTR**

Next attempt to compute the PFR trajectory from point F to point Q

For a PFR, $dc/d\tau = r(c)$

c_1 first:

$dc_1/d\tau = -c_1 - 20c_1^2$

$\int dc_1 / (-c_1 - 20c_1^2) = \int d\tau$

from calculus, $\int dx / x(ax + b) = 1/b \ln |(x / (ax + b)| + C$

a = -20, b = -1

$\int dc_1 / (-c_1 - 20c_1^2) = -\ln | c_1 / (-20c_1 - 1)| + C$ ($c_1 >= 0$ and $-20c_1 - 1 < 0$)

$= -\ln(c_1 / (20c_1 + 1)) + C = \tau$

$\ln(c_1 / (20c_1 + 1)) = C - \tau$

$c_1 / (20c_1 + 1) = e^{C - \tau}$

$c_1 = 20c_1 e^{C} e^{-\tau} + e^{C} e^{-\tau}$

$c_1 = e^{C} e^{-\tau} / (1 - 20e^{C} e^{-\tau})$

at τ=0, $c_1 = c_{10}$, so $C = \ln(c_{10} / (20c_{10} + 1))$ where c_{10} is the initial value of c_1 (in this case the feed point, but in the general case any point along the CSTR or DSR curve where a PFR trajectory could start from)

Substituting in the initial conditions and simplifying,

$c_1 = c_{10} / (20c_{10} + 1)e^{-\tau} - 20c_{10}$

However, computing c2, c3, and c4 became more difficult because the functions became difficult or impossible to integrate directly. For example,

$dc_3 / d\tau = 10c_1^2 = 10\ c_{10}^2 / [(20c_{10} + 1)e^{\tau} - 20c_{10}]^2$

Various integration methods such as substitution and integration by parts were attempted unsuccessfully. So, a differential equation solver called Polymath was used to compute the solutions, entering various initial conditions from the CSTR and DSR trajectory points and letting Polymath compute the points of the resulting PFR trajectories. These points were produced by Polymath as one text file per trajectory, which the application then read and parsed to get the points.

The system of ODE's is:

$dc_1 / d\tau = -c_1 - 20c_1^2$

$dc_2 / d\tau = c_1 - c$

$dc_3 / d\tau = 10\ c_1^2$

$dc_4 / d\tau = c_2$

The ouput points are stored in files c0.txt – c21.txt in the data directory for the project.

D.3 **DSR Trajectory**

From (Feinberg, 2000), the governing equation of a DSR is

$dc/d\tau = r(c) + \alpha(c)\ (c^0 - c)$

where c^0 is the side feed concentration, and $\alpha(c)$ is a function depending on the number of dimensions of c

c^0, the side feed concentration is (1,0,0), because the sample problem assumes an ample supply of the original feed supply is available to use as side feed (given)

The key is to find the critical $\alpha(c)$ function which will maximize the trajectory (ie, produce the trajectory lying in the AR, the so called critical DSR trajectory). From Feinberg, this is:

$$\alpha(c) = c_1 (20 c_1^3 c_2 – 80c_1^2c_2 - c_1^2 + 37c_1c_2 + c_1 + 2c_2) / 2 (c_1^2 – 2c_1 + 1) c_2$$

for a 3-dimensional system. Feinberg is using 3 dimensions for the sample problem because he is not interested in c_4.

The set of ODE's which were entered into Polymath are therefore:

$$dc_1/d\tau = -c_1 – 20c_1^2 + \alpha(c) (1 – c_1)$$

$$dc_2/d\tau = c_1 – c_2 + \alpha(c) (–c_2)$$

$$dc_3/d\tau = 10c_1^2 + \alpha(c) (-c_3)$$

where $\alpha(c)$ is given above

Derivation of c_4 stoichiometrically: By doing a mass balance on the system of chemical equations, we know that

$c_1 + c_2 + 2c_3 + c_4 = c_1^{feed} = 1$

So, with c_1,c_2,c_3 computed from Polymath and combined with c_4 computed stoichiometrically, we arrive at the full 4 dimensional DSR curve.

D.4 **PFR Trajectories from DSR**

We used the same system of ODE's in Polymath as in the PFR trajectories emanating from the CSTR curve to compute PFR trajectories emanating from the DSR curve. The initial conditions are simply now points from the DSR trajectory. These points were outputted by Polymath as one text file per trajectory, which our application then read and parsed to get the points.

The system of ODE's we used is:

$dc_1 / d\tau = -c_1 – 20c_1^2$

$dc_2 / d\tau = c_1 – c_2$

$dc_3 / d\tau = 10\ c_1^2$

$dc_4 / d\tau = c_2$

The output points are stored in files d0.txt – d25.txt in the data directory for the project.

VITA

NAME	Thomas Peterka
EDUCATION	University of Illinois at Chicago (UIC), Chicago, IL Bachelor of Science, Computer Science Engineering June, 1987
HONORS	Bell Honor Award for highest grade point average in the College of Engineering graduating class of 1987,5.0 / 5.0 GPA
RESEARCH	Research assistant, Electronic Visualization Laboratory (EVL) at UIC.
PROFESSIONAL AFFILIATIONS	Tau Beta Pi National Engineering Honor Society Phi Kappa Phi National Honor Society